Comparative secretome analysis of Colletotrichum falcatum identifies a cerato-platanin protein (EPL1) as a potential pathogen-associated molecular pattern (PAMP) inducing

Journal of Proteomics xxx (2017) xxx-xxx

Contents lists available at ScienceDirect

Journal of Proteomics

journal homepage: www.elsevier.com

Comparative secretome analysis of *Colletotrichum falcatum* identifies a cerato-platanin protein (EPL1) as a potential pathogen-associated molecular pattern (PAMP) inducing systemic resistance in sugarcane

N.M.R. Ashwin[a], Leonard Barnabas[a], Amalraj Ramesh Sundar[a, *], Palaniyandi Malathi[a], Rasappa Viswanathan[a], Antonio Masi[b], Ganesh Kumar Agrawal[c, d], Randeep Rakwal[c, d, e]

[a] *Division of Crop Protection, Indian Council of Agricultural Research - Sugarcane Breeding Institute, Coimbatore 641007, India*
[b] *Department of Agronomy, Food, Natural Resources, Animals and Environment, University of Padova, Padova 35020, Italy*
[c] *Research Laboratory for Biotechnology and Biochemistry, Kathmandu 13265, Nepal*
[d] *GRADE (Global Research Arch for Developing Education) Academy Private Limited, Adarsh Nagar-13, Birgunj, Nepal*
[e] *Faculty of Health and Sport Sciences, and Tsukuba International Academy for Sport Studies (TIAS), University of Tsukuba, Tsukuba, Ibaraki 305-8577, Japan*

ARTICLE INFO

Article history:
Received 14 January 2017
Received in revised form 12 April 2017
Accepted 17 May 2017
Available online xxx

Keywords:
Colletotrichum falcatum
Sugarcane
Secretome
Pathogen-associated molecular pattern (PAMP)
Effector
Systemic resistance

ABSTRACT

Colletotrichum falcatum, an intriguing hemibiotrophic fungal pathogen causes the devastating red rot disease of sugarcane. Repeated in vitro subculturing of *C. falcatum* under dark condition alters morphology and reduces virulence of the culture. *Hitherto*, no information is available on this phenomenon at molecular level. In this study, the in vitro secretome of *C. falcatum* cultured under light and dark conditions was analyzed using 2-DE coupled with MALDI TOF/TOF MS. Comparative analysis identified nine differentially abundant proteins. Among them, seven proteins were less abundant in the dark-cultured *C. falcatum*, wherein only two protein species of a cerato-platanin protein called EPL1 (eliciting plant response-like protein) were found to be highly abundant. Transcriptional expression of candidate high abundant proteins were profiled during host-pathogen interaction using qRT-PCR. Comprehensively, this comparative secretome analysis identified five putative effectors, two pathogenicity-related proteins and one pathogen-associated molecular pattern (PAMP) of *C. falcatum*. Functional characterization of three distinct domains of the PAMP (EPL1) showed that the major cerato-platanin domain (EPL1 Δ N1–92) is exclusively essential for inducing defense and hypersensitive response (HR) in sugarcane and tobacco, respectively. Further, priming with EPL1 Δ N1–92 protein induced systemic resistance and significantly suppressed the red rot disease severity in sugarcane.

Biological significance

Being the first secretomic investigation of *C. falcatum*, this study has identified five potential effectors, two pathogenicity-related proteins and a PAMP. Although many reports have highlighted the influence of light on pathogenicity, this study has established a direct link between light and expression of effectors, for the first time. This study has presented the influence of a novel N-terminal domain of EPL1 in physical and biological properties and established the functional role of major cerato-platanin domain of EPL1 as a potential elicitor inducing systemic resistance in sugarcane. Comprehensively, the study has identified proteins that putatively contribute to virulence of *C. falcatum* and for the first time, demonstrated the potential role of EPL1 in inducing PAMP-triggered immunity (PTI) in sugarcane.

Abbreviations: $(NH_4)_2SO_4$, ammonium sulphate;; BTH, benzothiadiazole; BYS1, *Blastomyces* yeast phase-specific protein 1; DAB, 3,3′-diaminobenzidine; EPL1, eliciting plant response-like protein 1; ETI, effector-triggered immunity; FDR, false discovery rate; GLHY, glycosyl hydrolase; H_2O_2, hydrogen peroxide; hpi, hours post-inoculation; HR, hypersensitive response; HYP, hypothetical; IMAC, immobilized metal affinity chromatography; kDa, kilo Dalton; LMW, low molecular weight; MEP1, metalloprotease; MLP, ML domain-containing protein; MW, molecular weight; NaCl, sodium chloride; NH_4HCO_3, ammonium bicarbonate; NPR1, non-expressor of pathogenesis-related genes 1; PAMP, pathogen-associated molecular pattern; PR proteins, pathogenesis-related proteins; PSM, peptide spectral match; PTI, PAMP-triggered immunity; PTM, post-translational modification; R proteins, resistance proteins; qRT-PCR, quantitative reverse transcription-PCR; SSP, small secreted protein; TFs, transcription factors

* Corresponding author at: Plant Pathology Section, Division of Crop Protection, ICAR-Sugarcane Breeding Institute, Coimbatore 641 007, Tamil Nadu, India.
Email address: rameshsundar_sbi@yahoo.co.in (A.R. Sundar)

http://dx.doi.org/10.1016/j.jprot.2017.05.020
1874-3919/

1. Introduction

Sugarcane is one of the most important commercial crops cultivated worldwide for the production of sugar, ethanol and other byproducts. *Colletotrichum falcatum*, a hemibiotrophic fungal pathogen causes a major devastating disease in sugarcane called red rot. *C. falcatum* primarily infects the sucrose-rich economically valuable stalk portion and thereby poses a huge challenge for sugarcane production in many tropical and subtropical countries [1]. The disease has been implicated in a considerable reduction of cane yield (30–100%) and sucrose recovery (25–75%) [2]. Breeding for durable red rot resistance is hampered by frequent emergence of new pathotypes of *C. falcatum*. On the other hand, the absence of whole genome information of this complex polyploidy crop strangled the efforts for molecular breeding [3]. Besides, disease management practices using fungicidal applications are not successful at grand growth phase of the crop. Hence, there is a pertinent demand for identification of effective compounds that can suppress red rot disease severity either by directly targeting *C. falcatum* or by inducing the innate immune system of sugarcane by priming.

During plant-pathogen interactions, plants recognize pathogens through perception of their conserved signatures called pathogen-associated molecular pattern (PAMP) and activates PAMP-triggered immunity (PTI) [4]. When the pathogens evade PTI through the secretion of effectors, plants employ R proteins (intracellular receptors) to recognize and activate effector triggered immunity (ETI) [5]. By mimicking the presence of a pathogen without real-time confrontation, these PAMPs themselves can potentially act as resistance inducers and could trigger active resistance of the host [6]. Nevertheless, based on the host genotype, certain effectors can also induce host resistance, which then can be designated as elicitors to that particular host genotype [7]. Generally, the process of enhancing the inherent defense potential of a plant by an external stimulus like biotic or abiotic inducing agents is called as induced resistance [8]. The active resistance thus inducible by priming with these elicitors would be systemic, durable and broad spectrum [9].

In sugarcane, suppression of red rot disease severity was demonstrated by priming using resistance inducers of abiotic origin, benzothiadiazole (BTH) and biotic origin, a glycoprotein elicitor isolated from *C. falcatum* cell wall [10,11,12]. Further, transcriptional profiling analyses showed upregulation of several defense-related transcription factors [13], phenylpropanoid pathway genes and resistant gene analogues at earlier stages of infection in the red rot susceptible cultivar, CoC 671 [14]. However, many other factors like cost effectiveness, and lack of protein sequence information have deterred scaled-up applications of BTH and glycoprotein elicitor, respectively for field situations. This has necessitated further hunting for identification of PAMPs and effectors of *C. falcatum* to accomplish sustainable crop protection and improvement through induced resistance and pathogen-derived resistance approaches, respectively.

Over the years, many reports have highlighted the influence of light on morphology, growth and reproduction of phytopathogens [15]. Further, it could act as an important modulator of fungal pathogenicity by either positively or negatively influencing the virulence of a pathogen [16]. Photoreceptor mediated signaling machinery that links the perception of light and virulence has been demonstrated phenotypically in *Botrytis cinerea* [17]. Yu et al. [18] reported that virulence of *Colletotrichum acutatum*, the causative agent of anthracnose in pepper plants was reduced, when cultured under dark condition.

C. falcatum, a predominant anamorphic fungus is generally cultured under light conditions for growth, maintenance, pathogenicity tests, etc. [19]. *Hitherto*, there is no detailed information on the changes in morphology, virulence and pathogenicity of *C. falcatum* cultured under dark conditions at molecular level. Hence, in this study, with an objective of identifying putative PAMPs and effectors of *C. falcatum*, a comparative secretome analysis of *C. falcatum* that were cultured under light and dark conditions was performed using 2-DE coupled with MS/MS. The abundance of identified proteins were validated at transcript level using qRT-PCR. Further, a putative PAMP identified in this analysis was investigated for its functional property as an elicitor of host defense in sugarcane and tobacco through a series of bioassays.

2. Materials and methods

2.1. Fungal culture and growth conditions

*C. falcatum Cf*671 (Microbial Type Culture Collection and Gene Bank, Chandigarh, India, accession number-12142), a highly virulent isolate was used for all experiments in this study. *Cf*671 was cultured separately under light and dark conditions in oat meal agar plates for three months by subculturing once in a fortnight. For light-culturing condition, the cultures were incubated at 28 °C with 14 h light (light intensity - 100 μmoles/m^2/s) and 10 h dark cycles (Model – MIR554, Panasonic Healthcare Co., Ltd., Gunma, Japan) and for dark-culturing condition, they were incubated at 28 °C without light. For secretome analysis, one mycelial disc of 5 mm diameter of light- and dark-cultures grown on agar plates were inoculated in individual 500 mL flasks each containing 150 mL of oat meal broth. Three flasks were inoculated individually for light- and dark-cultures with three independent biological replicates for each culture. The flasks were then incubated at 28 °C for 10 days in their respective light and dark conditions without agitation. Similarly, another set of flasks were inoculated and grown as mentioned above to ascertain their growth from their dry weight. To determine dry weight, the cultures were harvested by vacuum filtration, dried at 50 °C for 72 h and weighed in an electronic weighing machine.

2.2. Sugarcane cultivar and pathogen inoculation

Eight month old sugarcane cultivar CoC 671 (highly susceptible to red rot) grown in the institutional experimental farm (ICAR - Sugarcane Breeding Institute, Coimbatore, India) under natural climatic conditions was used for all the experiments. Plug method of inoculation [20] was used for inoculating the light- and dark-cultured *C. falcatum Cf*671. For all gene expression and pathogen biomass quantitation experiments, samples were collected at different time points, 0, 12, 24, 48, 72, 120 and 600 h post-inoculation (hpi) and stored at − 80 °C until further processing. Three samples representing each of the three biological replications were collected from individual time points. The sampling time point '0 h' represent mock inoculated control, for which sterile deionized water was used.

2.3. Secreted protein extraction, 1-DE and 2-DE

After 10 days of incubation, mycelial mats and spent medium were harvested using vacuum filtration method with 0.8 μm membrane filter (Supor® PES, Pall Corporation, USA). Mycelial retentates were stored at − 80 °C for gene expression analysis, whereas

collected spent media were further filtered using 0.45 μm membrane filter. Proteins were then precipitated from the filtrate and solubilized as described by Barnabas et al. [21]. Briefly, two volumes of 10% [w/v] TCA-acetone with 0.14% DTT were added to the filtered spent media and incubated at − 20 °C for 12 h. They were then centrifuged at 12,000 rpm for 15 min at 4 °C to collect the precipitated proteins in the form of a pellet. The pellets were then washed five times with ice cold acetone containing 0.07% DTT to remove excess TCA which is followed by freeze drying to remove residual acetone. Lyophilized protein powders were solubilized in a buffer containing 7 M urea, 2 M thiourea, 4% [w/v] CHAPS, 0.3% [w/v] DTT and 2% [v/v] IPG buffer pH 4–7 (GE Healthcare).

To precipitate the secreted proteins of dark-cultured *C. falcatum* in functionally active form for bioassays, ammonium sulphate ($(NH_4)_2SO_4$) was slowly added to the filtered spent medium up to 95% saturation while constantly mixing with a magnetic stirrer at 4 °C for 20 h. Precipitated proteins were then recovered by centrifugation at 12,000 rpm for 30 min and the pellets were resuspended in an assay buffer (50 mM Tris, 200 mM sodium chloride (NaCl), 10 mM β-Mercaptoethanol, 10% glycerol). Buffer exchanging was performed using 3 kDa Amicon ultra-15 centrifugal filters (Merck Millipore) to remove $(NH_4)_2SO_4$ salts from the assay buffer. Protein concentrations were quantified by Bradford method, using BSA as standards. The quality of the extracted proteins was analyzed using 1-DE (SDS-PAGE).

Proteins extracted in triplicates from three independent biological replicates using TCA-acetone method were subjected to 2-DE with two technical duplicates per biological replicate. Totally six replicates were analyzed per sample by 2-DE as described by Amalraj et al. [22]. Briefly, 300 μg of proteins were passively rehydrated onto 18 cm IPG strips with a pI range of 4–7 (GE Healthcare, Uppsala, Sweden). Isoelectric focusing was performed on Ettan IPGPhor II unit (GE Healthcare) until it attains 45000Vhrs. After focusing, the strips were reduced and alkylated with equilibration buffer I (50 mM Tris (pH 8.8), 6 M Urea, 30% [w/v] glycerol, 2% SDS and 1% DTT) and equilibration buffer II (50 mM Tris (pH 8.8), 6 M Urea, 30% [w/v] glycerol, 2% SDS and 2.5% iodoacetamide) for 20 min each. Second dimensional separation was performed in 12% SDS-PAGE gels in standard Tris-glycine buffer Ettan DALT-6 unit (GE Healthcare) and stained with colloidal Coomassie CBB staining with G-250 as described by Dyballa and Metzger [23].

2.4. Image capture and statistical analysis of protein spots

2-DE gel profiles were captured and digitized using ImageScanner III LabScan 6.0 (GE Healthcare) in compatible image formats (300 dpi, 16 bit, .tiff and .mel) for subsequent image analysis. For spot analysis, the images were imported into ImageMaster Platinum version 7 software (GE Healthcare). Parameters such as smooth, area, and saliency were adjusted appropriately to detect all the reliable spots. Gel to gel match was performed after land marking a few spots that were consistent in all the gel profiles. Thereafter, a spot-by-spot visual validation of detected spots was performed to increase the reliability of matching. To determine the abundance of spots, normalized spot volumes of consistent and reproducible spots (in at least four out of six replicates) were subjected to statistical analysis (Supplementary Table 1). The significance of each matched spots were statistically analyzed by Mann-Whitney *U* test using SPSS statistical software (version 21; IBM, NY, USA). Protein spots with p-value < 0.05 and with > 1.3 fold change by average normalized spot volume were manually excised from gels in duplicates for MS/MS analysis.

2.5. MS/MS analysis and database search

MS/MS analysis was performed as described by Barnabas et al. [24]. Briefly, excised spots were destained and washed four times with 50 mM ammonium bicarbonate (NH_4HCO_3) and 50% ACN, alternatively. They were then in-gel digested with 3 μL of 12.5 ng/μL sequencing-grade modified trypsin (Promega) in 50 mM NH_4HCO_3 at 37 °C, overnight. Subsequently, the peptides were extracted with 50% ACN and 0.1% TFA. Equal volumes of digested peptides and CHCA solution (5 mg/mL of CHCA in 70% ACN with TFA 0.1%) were mixed and spotted in duplicates (0.8 μl) onto a standard 386-well stainless steel MALDI target plate. MALDI TOF/TOF analyses were carried out using 4800 Plus MALDI TOF/TOF Analyzer (AB Sciex) and the spectra were collected in a data-dependent mode. Following a survey scan (MS), MS/MS was performed for 10 most abundant ions and all the spectra were exported for post-MS analysis. MS/MS spectra were searched against different *C. falcatum* databases using Peaks studio software (Version 8; Bioinformatics solution Inc., ON, Canada) supported with De novo, Peaks DB, PTM and Spider algorithms. *C. falcatum* databases employed for this analysis were translated TSA (transcriptome shotgun assembly) of *C. falcatum Cf*671 (Bioproject PRJNA272832), and the protein databases were constructed from whole genome shotgun assembly of *C. falcatum Cf*671 (Bioproject PRJNA272959) and *C. falcatum* MAFF306170 (Bioproject PRJNA262221) strains using AUGUSTUS gene prediction server (http://bioinf.uni-greifswald.de/augustus). Search parameters were set to 1 + for peptide charge state, 50 ppm for peptide mass tolerance, 0.3 Da for fragment mass tolerance and 1 for maximum missed cleavage. Carbamidomethylation (C) and oxidation (M) were set for fixed and variable modifications, respectively. Apart from these modifications, a maximum of three PTM predictions were allowed. Further, − 10lgP threshold and average local confidence threshold of de novo predictions were set to ≥ 50 for fetching peptide spectral matches (PSMs) and filtering false peptide spectral matches (PSM) so as to eliminate false positive identifications. False discovery rate (FDR) was estimated with decoy fusion method during Peaks DB search.

2.6. In silico analyses of identified proteins

Identified proteins were annotated using BLASTP search. To distinguish the identity of specific hypothetical proteins, numeric variables were used at the suffix of the abbreviation (HYP). Theoretical properties of identified proteins were predicted using ProtParam tool (ExPASy, Swiss Institute of Bioinformatics). Prediction of secreted proteins was performed with two classical secretory pathway prediction tools, viz., SignalP v 4.1 (www.cbs.dtu.dk/services/SignalP/) and TargetP v 1.1 (www.cbs.dtu.dk/services/TargetP/), and a non-classical secretory pathway prediction tool, SecretomeP v 2.0 (www.cbs.dtu.dk/services/SecretomeP/). Transmembrane region prediction and Hidden Markov Model (HMM)-based prediction of potential cleavage site were identified using TMHMM server v 2.0 (http://www.cbs.dtu.dk/services/TMHMM/) and SignalP v 3.0 (http://www.cbs.dtu.dk/services/SignalP-3.0/), respectively. Multiple sequence alignment and phylogenetic tree construction were performed with Clustal Omega (http://www.ebi.ac.uk/Tools/msa/clustalo/). Prediction of effector properties of secreted proteins were carried out using the tool, EffectorP (http://effectorp.csiro.au/) [25]. Modelling of three dimensional structure of protein was performed using SwissModel tool (https://swissmodel.expasy.org/interactive).

2.7. Biomass quantification and gene expression analysis using qPCR

For pathogen biomass quantification, total genomic DNA was extracted from the internodal region (covering approximately 2 cm above and below the site of pathogen challenge) of all the collected samples using CTAB method. In planta biomass of *C. falcatum* was quantified using an elongation factor gene, CfeEF1α by absolute quantification method [26]. Standard curve was generated from the amplification of CfeEF1α from ten-fold dilutions of *C. falcatum* DNA with a linear relationship (r^2) of 0.989. Quantitation cycle (Cq) values of test samples were then extrapolated against the standard curve to determine the quantity of pathogen biomass.

For gene expression analyses, total RNA was extracted from the internodal region as described above using TRI Reagent® (Sigma-Aldrich, USA) and then converted into cDNA using RevertAid™ H minus First Strand cDNA Synthesis Kit (Thermo Scientific, USA). To identify the most stable reference gene in sugarcane, three stable reference genes reported by Ling et al. [27] namely, elongation factor (ScEF1α), glyceraldehyde 3-phosphate dehydrogenase (ScGAPDH) and 25S ribosomal RNA (Sc25S rRNA) were evaluated using qRT-PCR. Among the three genes, ScEF1α was determined as the most stable reference gene by the tool NormFinder (NormFinder Excel add-in v 0.953). Similarly, the most stable reference gene of *C. falcatum* was identified as CfeEF1α, after evaluating two constitutive expressed genes viz., CfeEF1α and Cf Actin. The expression target genes of sugarcane and *C. falcatum* were normalized with ScEF1α and CfeEF1α reference genes, respectively. qPCR was performed in StepOnePlus™ Real-Time PCR (Applied Biosystems, CA, USA) using Power SYBR Green PCR Master Mix (Applied Biosystems). Expression of all the samples were examined in three biological replications with two technical duplicates each. Melt curve analysis was performed to verify amplification specificity of the target genes. Amplification efficiency of transcripts, primer sequences, amplicon length, and annealing temperature details were listed (Supplementary Table 2a). All the primers used in this study were designed using Primer BLAST software (http://www.ncbi.nlm.nih.gov/tools/primer-blast). Relative fold expression and respective standard deviation was determined by $2^{-\Delta\Delta CT}$ method. To determine the significance of expression between two groups, the ΔCt values of the transcripts were tested for normality and then statistically analyzed using Student's *t*-test by employing SPSS statistical software (version 21; IBM, NY, USA).

2.8. Cloning, expression and purification

To investigate the functional properties of identified proteins of interest, they were cloned in a pET 28a expression vector, which had 6X his and T7 fusion tags at N-terminal end of target genes and expressed in Rosetta™ 2(DE3)pLysS cells, followed by purification using immobilized metal affinity chromatography (IMAC). Briefly, the specific regions of interest to be cloned were amplified with appropriate gene specific primers flanked with the restriction sites viz., *Eco*RI and *Hin*dIII with stuffer bases at 5′ region (Supplementary Table 2b). The inserts and the vector were separately double digested with *Eco*RI and *Hin*dIII (Thermo Scientific, USA) as per manufacturer's protocol. Purified digested inserts and vectors were ligated with T4 DNA Ligase (Invitrogen, USA), and transformed into Rosetta™ 2(DE3)pLysS cells. Veracity of positive clones grown on kanamycin Luria Bertani (LB) agar plates were tested by colony PCR, restriction digestion and by Sanger sequencing.

For protein expression, the positive clones of Rosetta™ 2(DE3)pLysS cells were induced at 0.5 OD with 0.5 mM Isopropyl β-D-1-thiogalactopyranoside (IPTG) at 30 °C for 4 h. The cells were then pelleted down at 6, 000 rpm for 5 mins and resuspended in 0.1 volume of extraction buffer (50 mM Tris, 200 mM NaCl, 10 mM β-Mercaptoethanol, 10% glycerol). After three cycles of freeze-thaw in liquid nitrogen, the resuspension was sonicated at 10 s pulse on, 10 s pulse off for 1 min at 30% amplitude. The lysates were then centrifuged at 13, 000 rpm for 10 min at 4 °C to collect the supernatant. Recombinant his-tag proteins were then purified through Ni-Sepharose 6 Fast Flow column (GE Healthcare) by eluting them in a linear gradient of extraction buffer containing 500 mM imidazole from 0 to 500 mM in 30 min using a low pressure chromatography system (BioLogic™ LP System, Biorad, USA). The quality of protein extracts and purified fractions were analyzed using 13% SDS-PAGE at every step. The purified fractions were immediately buffer exchanged with assay buffer (50 mM Tris, 200 mM NaCl, 10 mM β-Mercaptoethanol, 10% glycerol) using 3 kDa Amicon ultra-15 centrifugal filters (Merck Millipore) to remove imidazole and to reduce the salt concentration. The fractions were further purified by size exclusion chromatography using Sephacryl S100 HR column using a low pressure chromatography system (BioLogic™ LP System, Biorad, USA).

2.9. Western blot

Western blot analysis of purified recombinant proteins were carried out as described by Ramesh Sundar et al. [10]. Briefly, purified proteins in electrophoresed gels were electroblotted in an activated PVDF membrane (0.2 μm) by semidry transfer method using Trans-Blot® SD Semi-Dry Transfer Cell (Biorad, USA). After blocking with skimmed milk powder, the membrane was incubated with a recombinant protein specific primary antibody (T7 Tag Monoclonal antibody, Merck Millipore). After three washes, the membrane was incubated with the secondary antibody (Goat Anti-Mouse IgG-Alkaline Phosphatase antibody, Sigma-Aldrich) and developed with the substrate, 5-Bromo-4-chloro-3-indolyl phosphate (BCIP) in conjunction with nitro blue tetrazolium (NBT). For activity assays, the N-terminal his-tag of purified proteins were removed using Thrombin CleanCleave™ Kit (Sigma-Aldrich) through centrifugation recovery method as per manufacturer's instructions.

2.10. Physical characterization of recombinant proteins

To resolve the dimeric and tetrameric forms of recombinant proteins, they were subjected to thermal stress up to 95 °C for 5 min and strong reducing environment with 700 mM of β-Mercaptoethanol or 300 mM of DTT. Subsequently, they were analyzed by Western blot for detection of dimeric and tetrameric forms. To observe the self-assembling property of recombinant proteins, the protein solution (in assay buffer) were gently pipetted up and down in a micro tube and placed a drop in a glass slide under room temperature for 2 h [28]. After 2 h, the drops were examined under light microscope.

2.11. Analysis of extracellular pH and hydrogen peroxide (H_2O_2) production in sugarcane suspension cell culture

Sugarcane suspension culture was established from friable embryogenic calli of CoC 671 for bioassays. Native secreted proteins of dark-cultured *C. falcatum* was fractionated with 30 kDa Amicon ultra-15 centrifugal filters (Merck Millipore) and the flow through low molecular weight (LMW) fraction was further concentrated with

3 kDa Amicon ultra-15 centrifugal filters, which served as a positive control for the assays involving recombinant proteins, whereas for negative control, only assay buffer was used. After treatment with 50 µL of optimum concentration of native LMW and purified recombinant proteins, extracellular pH changes in the sugarcane suspension cells were observed at different time points (from 0 to 3 h after treatment) as described by Chen et al. [29]. For detection of H_2O_2 production in suspension culture, 10 µL/mL of 3,3′-Diaminobenzidine (DAB) tetrahydrochloride hydrate (Sigma-Aldrich) (1 mg/mL) solution, pH 3.8 was added immediately after treatment with recombinant proteins and observed under light microscope after 24 h of incubation under dark condition. All the bioassays were repeated three times to verify the reproducibility and only the representative images were presented.

2.12. Hypersensitive response (HR) assay and detection of H_2O_2 production on tobacco leaves

HR assay and detection of H_2O_2 production on *Nicotiana tabacum* leaves were carried out as described by Chen et al. [29]. Briefly, 50 µL of optimum concentration of recombinant proteins were infiltrated at the adaxial side on *N. tabacum* leaves using a needleless syringe and documented after 24 h for HR response. Then, the leaf discs (approximately 2 cm radius around the site of infiltration) were excised and incubated in DAB solution (1 mg/mL) solution under dark condition for 8 h. Stained leaf discs were bleached in 95% boiling ethanol for 20 mins to remove chlorophyll contents and stored at 70% glycerol for examination under light microscope. All the bioassays were repeated for three times to verify the reproducibility and only the representative images were presented.

2.13. Priming and detached leaf assay

To evaluate priming and co-infiltration effect of recombinant proteins, detached leaf assay was carried out as described by Viswanathan et al. [30]. For priming, eight month old CoC 671 canes were foliar sprayed with an optimum concentration of recombinant proteins (25 mL/cane) for two times at ten days interval using a 500 mL handheld sprayer. After two weeks of foliar spray, primed canes were inoculated with light-cultured *Cf671* by plug inoculation method and the samples from stalk portion were collected at different time points (0, 12, 24, 48, 72, 120 and 600 hpi) and stored at − 80 °C until further processing for pathogen biomass quantitation and gene expression analysis.

On the other hand, matured third leaves of primed canes were detached and the bottom portion of the leaves (25 cm) were cut and gently washed with deionized water. Since, sugarcane leaf surfaces are covered with thick cuticle layer enriched with waxes, minor injuries (5 pinpricks in app. 3 mm^2 area) were made at the middle portion of the leaves on both sides of midrib to facilitate the penetration of infection peg. After that, 50 µL of light-cultured *Cf671* spores (10^6 spores/mL) were inoculated and incubated in an illuminated growth chamber (Model - E41L2, Percival Scientific Inc., IA, USA) at 28 °C with 60% humidity in 14 h light (light intensity – 600 µmoles/m^2/s) and 10 h dark cycling conditions. For co-infiltration with recombinant proteins, desired concentration of recombinant protein solution was prepared with deionized water and subsequently, *Cf671* spore suspension was prepared with the recombinant protein solution, and inoculated on detached untreated leaves as described above. Germination and formation of infection structures were observed under light microscope at 24 hpi, and lesion development from the point of inoculation was observed at 72 hpi. Three independent replications were maintained for each set of treatments.

3. Results and discussion

3.1. Influence of light on morphology and pathogenicity of C. falcatum

To study the effect of light on morphology and pathogenicity of *C. falcatum*, it was separately subcultured under light and dark conditions for three months. While the morphology of light-cultured *C. falcatum* remained unaltered, the morphology of dark-cultured *C. falcatum* has altered from grey to pure white dense cottony mycelium with no obvious sporulation on culture plates (Fig. 1A). Generally, light influences sporulation and pigmentation properties of fungal cultures [31]. In some cases, excess light had induced dark pigmentation and resulted in retardation of growth [17]. In our case, neither the growth

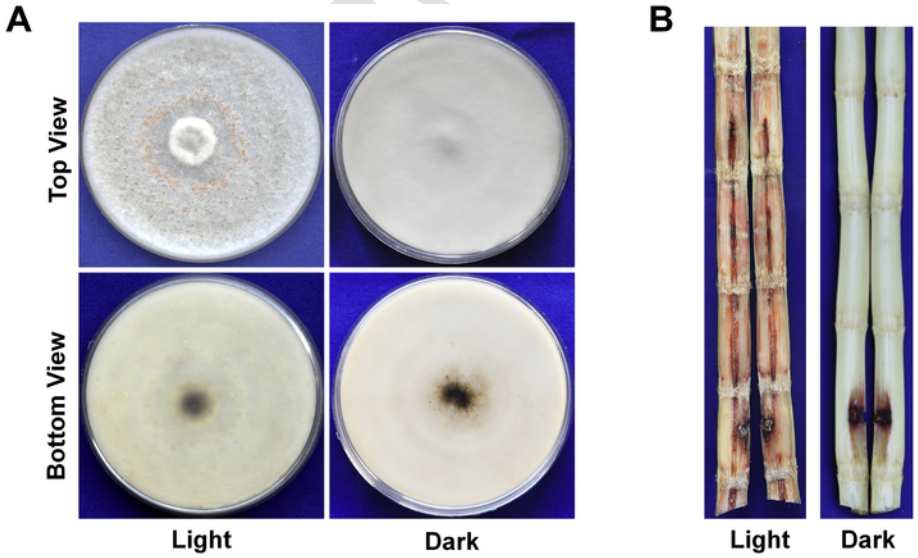

Fig. 1. Effect of in vitro culturing of *C. falcatum* under light and dark conditions. A) Culture morphology after 14 days of incubation; B) Phenotyping of disease severity on cane stalks (cv. CoC 671) at 25 days post-inoculation with light- and dark-cultured *C. falcatum*.

nor the pigmentation at the bottom of culture plates showed significant difference between light- and dark-cultured *C. falcatum*, except sporulation. Further, pathogenicity tests of these cultures on red rot susceptible cultivar, CoC 671 resulted in loss or complete reduction of virulence in dark-cultured *C. falcatum*, when compared to the light-cultured ones (Fig. 1B). Conventionally, *C. falcatum* cultures were classified into light and dark races, based on the pigmentation and color of mycelium, wherein light race cultures exhibited higher virulence over the dark race cultures [32]. However, in this study, the influence of light on pathogenicity without affecting pigmentation pattern has suggested that the absence of light might have affected other physiological processes related to the production or expression of virulence determinants, beyond pigmentation.

3.2. Comparative secretome analysis of light- and dark-cultured C. falcatum

Generally, PAMPs are conserved biomolecular signatures of a pathogen that can be recognized by plants. Most of these signatures are either present in the form of proteins, polysaccharides, lipids, lipoproteins, etc. in the surfaces of cell wall and plasma membrane or constitutively secrete in extracellular spaces in the form of proteins. These biomolecules are mostly essential for pathogen fitness or survival [7]. On the other hand, effectors are virulence determinants that are secreted in the form of proteins, either constitutively or only during specific developmental stages to aid pathogenicity by suppressing host defense [33]. Hence, to identify the bilateral targets viz., putative PAMPs and effectors of *C. falcatum* with a single approach, a comparative secretome analysis of *C. falcatum* that were cultured under light and dark conditions was performed using 2-DE coupled with MS/MS. Before extraction of secreted proteins, an assessment of the growth of light- and dark-cultured *C. falcatum* from their dry weight biomass showed no differences.

Quantification of the secreted proteins that were extracted from three independent biological replicates of light- and dark-cultured *C. falcatum* showed no considerable difference between them. Extracted proteins were resolved using 2-DE in a pH range of 4–7. Visually, the 2-DE profiles showed major alterations in protein spot abundances in the region of LMW proteins ranging from 10 to 30 kDa (Fig. 2). A comparative analysis of these 2-DE profiles using ImageMaster Platinum version 7 software (GE Healthcare) showed that around 70–75 distinct protein spots were matched in all the biological and technical replicates, and between samples with high reproducibility (Supplementary Table 1). Further, statistical analysis of abundance of protein spots using Mann-Whitney *U* test (SPSS statistical software v21, IBM, NY, USA) indicated significant alterations in the abundance of 9 protein spots, while 2 protein spots were found to be exclusively secreted. These protein spots were subjected to MALDI-TOF/TOF and the obtained mass data was used to perform database search using Peaks studio software (Version 8; Bioinformatics solution Inc., ON, Canada) against *C. falcatum* specific databases as a reference (Table 1). Unique PSMs, protein and peptide scores of identified proteins with an overall FDR of 0.0% (Supplementary Fig. 1) were listed in Supplementary Table 3. Among the 9 differentially abundant protein spots, seven spots that were less abundant in the dark-cultured *C. falcatum* sample were identified as metalloprotease (MEP1), small secreted protein (SSP), ML domain-containing protein (MLP), putative glycosyl hydrolase (GLHY), *Blastomyces* yeast phase-specific protein 1 (BYS1) family protein and two protein species representing a single hypothetical protein (HYP2). Interestingly, the two protein spots that were highly abundant in the dark-culture represented the same protein, eliciting plant response-like protein (EPL1). Besides these differentially abundant protein spots, the one that was secreted exclusively in dark-culture was identified as a hypothetical protein (HYP1), whereas the other one that secreted exclusively in light-culture was identified as the second protein species of BYS1. Notably, among the 11 protein spots identified in this investigation, three proteins viz., BYS1, HYP2 and EPL1 represented two different protein spots each.

3.3. In silico analysis of identified proteins

To validate the secretory nature of identified proteins, classical and non-classical secretory pathway prediction tools were employed. This analysis revealed that except the MLP protein, all other identified proteins were predicted to be secreted by either classical or non-classical secretory pathways (Table 1). Full length amino acid sequences of identified proteins, and their predicted signal peptides and other targeting regions were tabulated in Supplementary Table 4. Many secretome studies involving plants and fungi reported a considerable percentage of secreted proteins, which were not predicted to be secreted by both classical and non-classical secretion based predic-

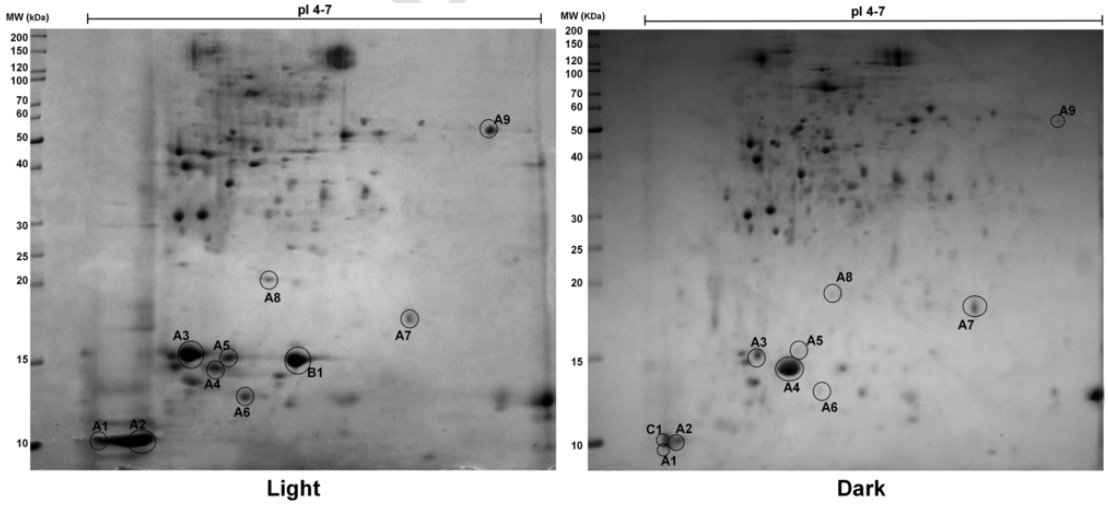

Fig. 2. Representative 2-DE profiles of in vitro secretome of light- and dark-cultured *C. falcatum*. Encircled protein spots were analyzed by MALDI-TOF/TOF. Labelled letters indicates A - Common spots, B - Repressed, C - Induced.

Table 1
Identification of differentially abundant secreted proteins of *C. falcatum* when subculturing under light and dark conditions.

S. No.	Spot ID[a]	Accession ID (TSA)[b]	Accession ID (WGS)[c]	Protein description[e]	Species (Accession ID)[e]	− 10lgP score[f]	Coverage %	No. of unique peptides	Fold change	*p* Value (Mann-Whitney *U* test)	Secretory prediction[g]	Theoretical MW/pI (with SP)[h]	Theoretical MW/pI (without SP)[i]
1	A1	9438	LPVI01003569.1	Metalloprotease (MEP1)	*Colletotrichum sublineola* (KDN66198.1)	364	75	3	− 1.3	0.025	+ +	11.04/9.74	9/9.1
2	A2	769	LPVI01002046.1	Small secreted protein (SSP)	*Colletotrichum incanum* (KZL82195.1)	208	29	3	− 6.85	0.004	+ +	15.7/5.18	13.6/5.18
3	A3	3022	LPVI01002063.1	Hypothetical protein (HYP2)	*Colletotrichum sublineola (*KDN59943.1)	372	57	5	− 5.69	0.004	+ +	14.5/4.8	12.1/4.64
4	A4	798	LPVI01003891.1	Eliciting plant response-like protein (EPL1)	*Colletotrichum orbiculare (*ENH79784.1)	423	49	6	7.53	0.004	− −, +*	22.8/7.81	12.5/4.88
5	A5	301	Scaffold_230[d]	Bys1 family protein (BYS1)	*Colletotrichum graminicola* (XP_008095376.1)	398	36	6	− 5.89	0.004	− +, +*	17.9/9.37	14.1/5.24
6	A6	3022	LPVI01002063.1	Hypothetical protein (HYP2)	*Colletotrichum sublineola* (KDN59943.1)	236	40	4	− 3.27	0.004	+ +	14.5/4.8	12.1/4.64
7	A7	798	LPVI01003891.1	Eliciting plant response-like protein (EPL1)	*Colletotrichum orbiculare* (ENH79784.1)	263	42	7	1.3	0.025	− −, +*	22.8/7.81	12.5/4.88
8	A8	485	LPVI01003093.1	ML domain-containing protein (MLP)	*Colletotrichum graminicola* (XP_008094990.1)	210	32	3	− 2.22	0.004	− −, −*	22.1/5.25	–
9	A9	8863	LPVI01003605.1	Putative glycosyl hydrolase family 10 (GLHY)	*Colletotrichum sublineola* (KDN64203.1)	560	44	10	− 5.78	0.004	+ +	42.7/6.28	41.4/6.3
10	B1	301	Scaffold_230[d]	Bys1 family protein (BYS1)	*Colletotrichum graminicola* (XP_008095376.1)	389	47	5	#	–	− +, +*	17.9/9.37	14.1/5.24
11	C1	10,773	LPVI01004073.1	Hypothetical protein (HYP1)	*Colletotrichum graminicola* (XP_008096807.1)	218	32	2	@	–	+ +	12.8/6.03	10.4/7.7

#Protein secreted exclusively by light-cultured *C. falcatum*.
@Protein secreted exclusively by dark-cultured *C. falcatum*.

[a] Spot IDs correspond to spots encircled in representative 2DE gel profile.

[b] Transcriptome shotgun assembly ID of *C. falcatum Cf*671 (Bioproject PRJNA272832) that corresponds to the protein hit.

[c] Genbank accession ID from the whole genome shotgun sequences of *C. falcatum Cf*671 (Bioproject PRJNA272959) that corresponds to the protein hit.

[d] Scaffold ID from the whole genome assembly of *C. falcatum* MAFF306170 (Bioproject PRJNA262221) that corresponds to the protein hit.

[e] Descriptions of the identified proteins based on BLASTP search against non-redundant protein database.

[f] Protein identification score (− 10lgP) as calculated from the peptide scores by Peaks database.

[g] Series of symbols (+/−) indicate the prediction of classical protein secretion by SignalP v 4.1, TargetP v 1.1, respectively, while (+* / −*) indicates prediction of non-classical protein secretion by SecretomeP v 2.0.

[h] Values indicating theoretical molecular weight/pI are inclusive of signal peptides.

[i] Values indicating theoretical molecular weight/pI are excluding signal peptides.

tion tools, similar to the case of MLP protein. To categorize these kinds of proteins, Saunders et al. [34] created a new class called atypical secreted proteins and classified the proteins like MLP and phosphatidyl ethanolamine-binding protein under this category.

Beside signal peptide analysis, the theoretical molecular weight (MW) and pI of all identified proteins with and without signal peptides were predicted using ProtParam tool to corroborate them with the observed 2-DE protein profiles. The theoretical MW and pI of most of the identified proteins were almost corroborating with the apparent MW and pI in 2-DE profiles, except for BYS1, HYP2 and EPL1 proteins, which were represented by more than one protein species. The observed discrepancy could be due to any of the cellular processes like post-transcriptional modification (alternative splicing), post-translational modification (PTM), etc., which can be determined only through a series of appropriate transcriptomic and proteomic experiments [35,36].

3.4. Analysis of transcriptional abundance of identified proteins and protein species

Abundance of protein spots were verified at transcriptional level using qRT-PCR. Relative transcriptional expression analysis of candidate identified proteins, viz., MEP1, SSP, MLP, GLHY, HYP1 and BYS1 exhibited a similar trend of fold differences of relative expression, compared to its corresponding abundance of protein spots (Fig. 3). Since, the protein spots A5 and B1 with different spot abundances and pI, but with same MW, (Fig. 2) represented the same protein, BYS1, transcriptional expression analysis was performed with only one primer set (qBYS1). Mostly, this kind of pI shift could be due to PTM of proteins [37]. A deeper analysis of PSMs of these two identified proteins spots with PTM algorithm in Peaks studio software (Version 8; Bioinformatics solution Inc., ON, Canada) suggested that the protein spot, A5 might have got phosphorylated and shifted to-

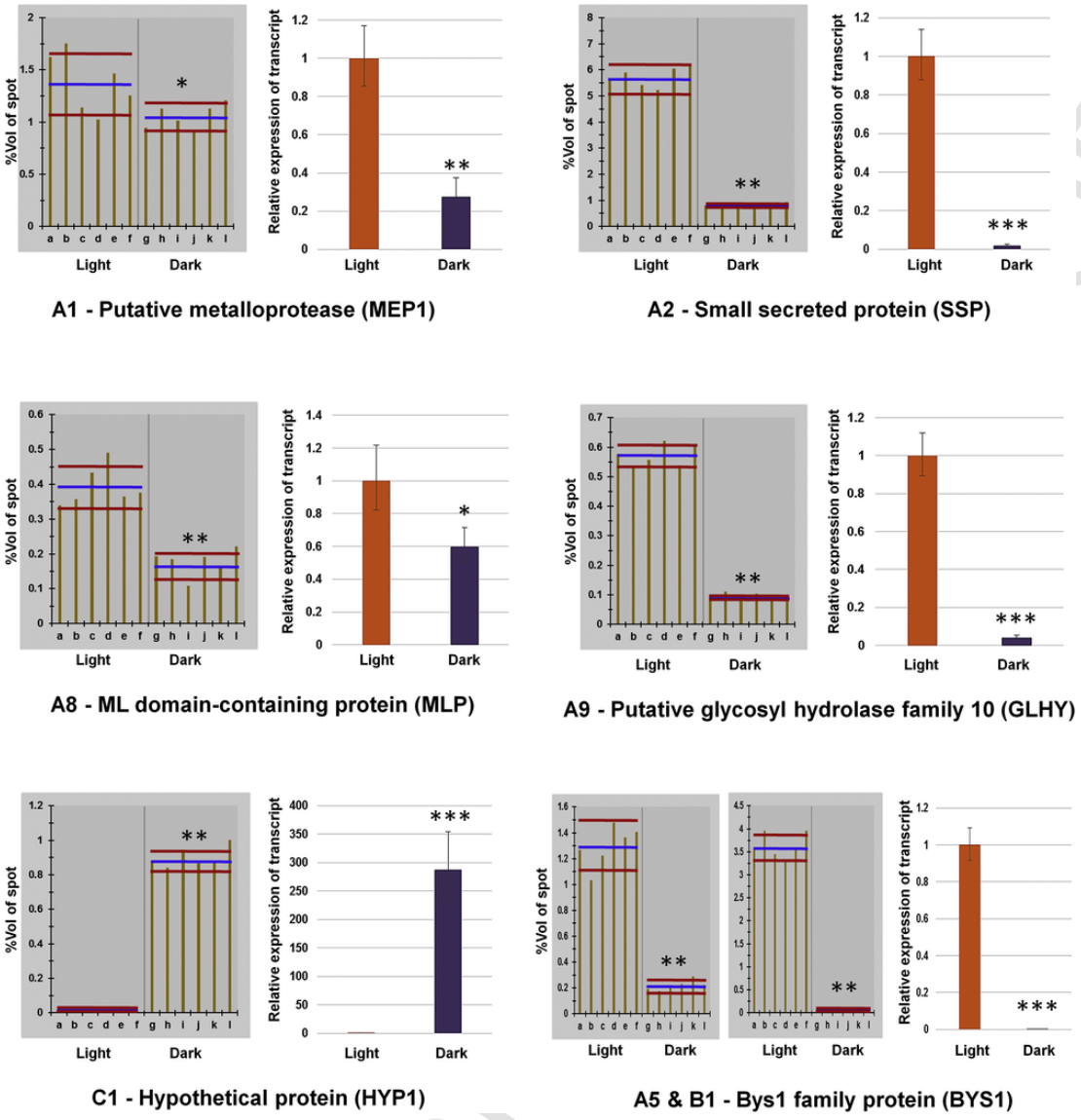

Fig. 3. Comparative analysis of abundance of protein spots and their corresponding expression of RNA transcripts. Letters in X-axis of proteins spot abundance indicate replications (a–f and g–l indicates spots from three biological replicates with two technical replicates each of light- and dark-cultured *C. falcatum* secretome samples, respectively). Blue and red horizontal lines in abundance of spots represent class mean and class mean squared deviation and asterisks indicate statistical significance as determined by Mann-Whitney *U* test (*$p < 0.05$; **$p < 0.01$; ***$p < 0.001$). Relative transcript expression with error bars indicate standard deviation of three biological replicates with two technical replicates each. Asterisks over error bar indicate significantly different as measured by Student's *t*-test (*$p < 0.05$; **$p < 0.01$; ***$p < 0.001$). (For interpretation of the references to color in this figure legend, the reader is referred to the web version of this article.)

wards acidic region (Supplementary Fig. 2). However, the phosphorylation was predicted with only one PSM of A5 spot and so, the possibilities of other PTMs cannot be ruled out.

The transcriptional validation of the remaining two identified proteins, HYP2 and EPL1, were relatively complex, because each protein represented two different protein species with different MW and pI. Therefore, the protein sequences were analyzed with various in silico tools to discover the possibilities of production of different protein products from the same gene and accordingly, different set of primers were designed to validate the assumptions at the transcript level. First, the PSMs of A3 and A6 spots were graphically mapped to the full length HYP2 (HYP2FL) amino acid sequence, which provided a vital clue on differences in coverage. Specifically, the A3 spot had 17% more coverage in the downstream of signal peptide (N-terminal region), when compared to the A6 spot (Fig. 4A and B). This has strengthened the hypothesis of alternative splicing event in HYP2 gene. Therefore, the HYP2FL sequence was virtually segmented into three distinct regions viz., signal peptide, putative splicing region and the main hypothetical domain. Based on this hypothesis, different set of primers were designed to verify the expression of different gene products of HYP2 (Fig. 4C and D). In contrary to the hypothesis, the relative expression of all the three different gene products remained unaltered and so, the chance of a splicing event of HYP2 was ruled out (Fig. 4E). However, the significant fold differences of transcript expression and spot abundances of the two protein species were comparably equal. Hence, the possibilities of other events like protease-catalyzed splicing [38] or intein splicing [39], cannot be ruled out for A6 spot.

On the other hand, the protein species of EPL1 were also analyzed with various in silico tools to predict signal peptide, cleavage site and

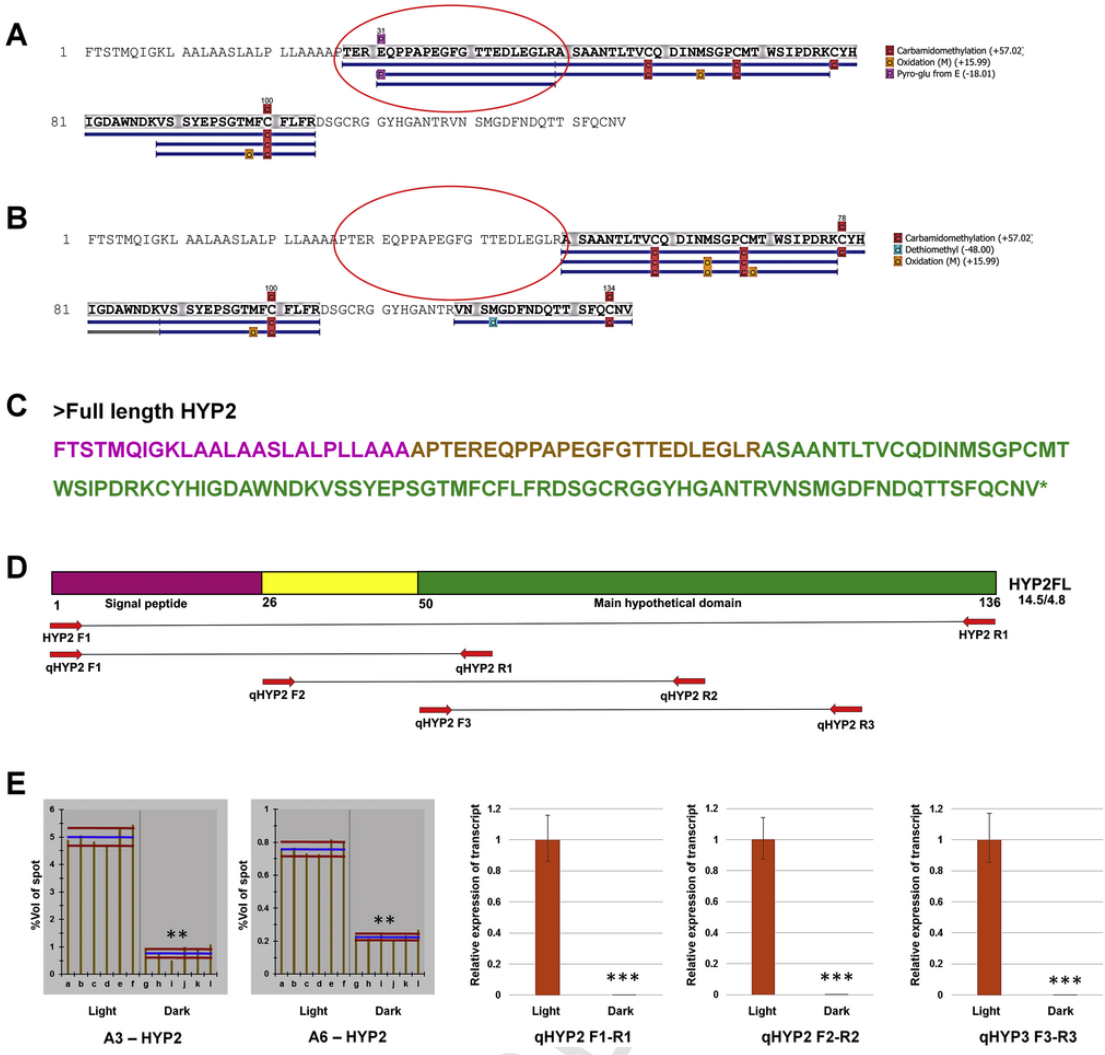

Fig. 4. Analysis of putative protein species of Hypothetical protein (HYP2). A) PSM coverage of spot A3 – HYP2 protein; B) PSM coverage of spot A6 – HYP2 protein. Encircled regions indicate the differences in coverage between A3 and A6 spots; C) Full length protein sequence of HYP2. Residues in different colors indicate putatively distinct domains; D) Putative domains of HYP2 protein and the sets of primers used to amplify distinct regions of HYP2 using qRT-PCR; E) Abundance of protein spots of HYP2 – A3 and A6, and relative expression of RNA transcripts that specifically amplify distinct regions of HYP2 using qRT-PCR. Letters in X-axis of proteins spot abundance indicate replications (a–f and g–l indicates spots from three biological replicates with two technical replicates each of light- and dark-cultured *C. falcatum* secretome samples, respectively). Blue and red horizontal lines in abundance of spots represent class mean and class mean squared deviation and asterisks indicate statistical significance as determined by Mann-Whitney *U* test (*$p < 0.05$; **$p < 0.01$; ***$p < 0.001$). Relative transcript expression with error bars indicate standard deviation of three biological replicates with two technical replicates each. Asterisks over error bar indicate significant difference as measured by Student's *t*-test (*$p < 0.05$; **$p < 0.01$; ***$p < 0.001$). (For interpretation of the references to color in this figure legend, the reader is referred to the web version of this article.)

transmembrane regions. Even though, SignalP v 4.1 did not detect any signal peptide in full length EPL1 (EPL1FL) (Supplementary Fig. 3a), TMHMM server v 2.0 and SecretomeP v 2.0 indicated a maximum probability for extracellular secretion (Supplementary Fig. 3b). Further mining of EPL1 with Hidden Markov model (HMM) based signal peptide prediction using SignalP server v 3.0, detected a potential cleavage site at the residue of 74 (Supplementary Fig. 3c). Intriguingly, the remaining truncated sequence (75–212 residues) indicated the presence of a signal peptide with a potential cleavage site at 92nd residue (Supplementary Fig. 3d). Localization prediction of this EPL1FL with TargetP server v 1.1 indicated that the N- terminal residues from 1 to 92 represents mitochondrial membrane targeting sequence (Supplementary Fig. 4a). However, graphical mapping of PSMs of A4 and A7 spots to EPL1FL indicated that both had a similar coverage in the region excluding the residues of 1–92 (Supplementary Fig. 4b and c). Based on these in silico analysis, EPL1FL was virtually segmented into three putative domains viz., putative signal peptide 1, signal peptide 2 and main cerato-platanin domain, which can hypothetically result into two to three gene products viz., EPL1FL, EPL1 Δ N1–74 and EPL1 Δ N1–92 (Fig. 5A and B). Transcriptional expression of these three products by qRT-PCR showed that the expression of qEPL1F1-R1 was completely different from the expression of qEPL1F2-R2 and qEPL1F3-R3 in both light- and dark-cultures (Fig. 5C). These results have confirmed that CfEPL1 encoded two different gene products, EPL1FL and EPL1 Δ N1–74, which might have resulted in two protein species, A7 and A4 spots, respectively. In other words, signal peptide present in EPL1 Δ N1–74 might have got cleaved and represented the A4 spot in the form of EPL1 Δ N1–92. Besides, the abundance of the protein spots, A7 and A4, were also comparable to the expression of EPL1FL and EPL1 Δ N1–74 transcripts, respectively, in both light- and dark-cul-

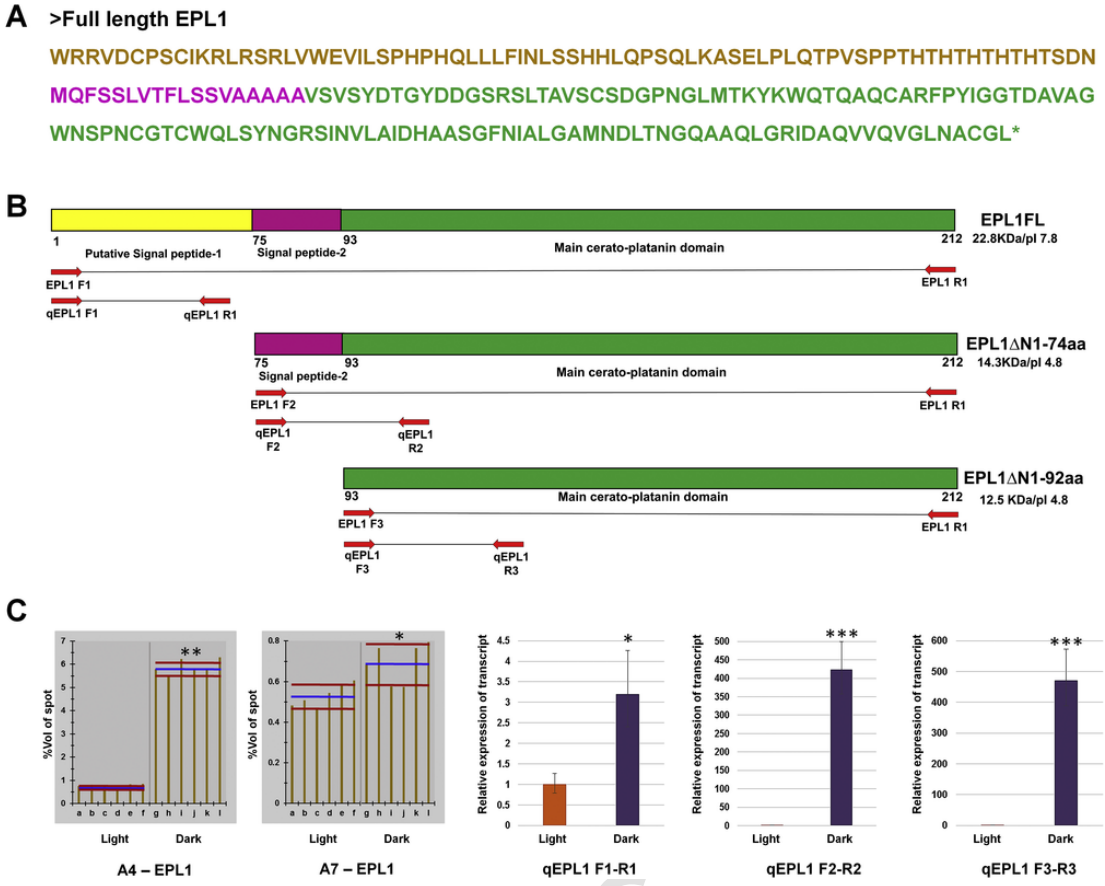

Fig. 5. Analysis of putative protein species of eliciting plant response-like protein (EPL1). A) Full length protein sequence of EPL1. Residues in different colors indicate putative distinct domains; B) Putative domains of EPL1 protein, representation of domain deletion constructs and the sets of primers used to amplify distinct regions of EPL1; C) Abundance of protein spots of EPL1 – A4 and A7, and relative expression of RNA transcripts that specifically amplify distinct regions of EPL1 using qRT-PCR. Letters in X-axis of proteins spot abundance indicate replications (a-f and g-l indicates spots from three biological replicates with two technical replicates each of light- and dark-cultured *C. falcatum* secretome samples, respectively). Blue and red horizontal lines in abundance of spots represent class mean and class mean squared deviation and asterisks indicate statistical significance as determined by Mann-Whitney *U* test (*$p < 0.05$; **$p < 0.01$; ***$p < 0.001$). Relative transcript expression with error bars indicate standard deviation of three biological replicates with two technical replicates each. Asterisks over error bar indicate significant difference as measured by Student's *t*-test (*$p < 0.05$; **$p < 0.01$; ***$p < 0.001$). (For interpretation of the references to color in this figure legend, the reader is referred to the web version of this article.)

tures of *C. falcatum*. Altogether, it was evident that the gene, EPL1 produced two transcripts or isoforms, EPL1FL and EPL1 Δ N1–74.

3.5. Functional significance of identified proteins

Light affects the transcription of many photoreceptor-related genes in fungi, which in turn influences the physiological processes like conidiation and pigmentation, and thereby pathogenicity [16]. Virulence factors that drive the pathogenicity exist in the form of proteins and metabolites. Secreted proteinaceous virulence factors, often referred to as effectors, determine the outcome of any plant-pathogen interaction. In the present study, absence of light has altered the abundance of 11 proteins. A prediction analysis of these identified proteins using EffectorP tool revealed that 8 out of the 11 proteins possessed effector properties and had a higher probability to be classified as effectors (Table 2). In addition to the common effector properties like small size and cysteine-richness, EffectorP tool predicts effectors on the basis of robust signals and sequence-derived properties with a sensitivity of > 80% from a fungal secretome [25]. Since, 6 out of these 8 predicted effectors were highly abundant on light-cultured *C. falcatum*, it was contemplated that these predicted effectors could be directly related to pathogen virulence, which warrant a deeper insight into the functional significance of individual proteins.

Table 2
Prediction of effector properties of identified proteins using EffectorP tool.

S. No.	Target Protein	With Signal peptide		Without Signal peptide	
		EffectorP prediction	Probability	EffectorP prediction	Probability
1	Metalloprotease (MEP1)	Effector	0.997	Effector	0.997
2	Small secreted protein (SSP)	Non-effector	0.981	Non-effector	0.868
3	Bys1 family protein (BYS1)	Effector	0.964	Effector	0.901
4	ML domain-containing protein (MLP)	Effector	0.976	–	–
5	Glycosyl hydrolase family 10 (GLHY)	Non-effector	1.000	Non-effector	1.000
6	Hypothetical protein (HYP1)	Effector	0.940	Effector	0.978
7	Hypothetical protein (HYP2)	Effector	0.935	Effector	1.000
8	Eliciting plant response-like protein (EPL1)[a]	Non-effector	0.679	Effector	0.701

[a] For prediction of effector properties of EPL1, EPL1FL and EPL1 Δ N1–92 were used in place of with and without signal peptide, respectively.

Among the differentially abundant proteins, Metalloprotease (MEP1) was found to be just 1.3 fold less abundant in the dark-culture of *C. falcatum*. Fungal metalloproteases are the proteases classified under the family of fungalysins (http://merops.sanger.ac.uk/). The major role of this protein is to catalyze the enzymatic hydrolysis of proteins with the help of a metal ion bound to the catalytic center of this protein. Many fungal metalloproteases have been reported to play a major role in pathogenicity, especially at the earlier stages of infection as effectors [40]. Among them, a well-studied metalloprotease is Avr-Pita effector (a zinc binding metalloprotease) from the rice blast fungus, *Magnaporthe oryzae*, against which the host resistance gene, Pi-ta activates ETI [40,41]. In maize, the higher expression of MEP1 of *Colletotrichum graminicola* at biotrophic phase has been suggested to play a major role in infection and anthracnose development [42]. Further, functional studies with mutants of MEP1 exhibited retarded disease development, which demonstrated its role in virulence [43]. Therefore, the MEP1 of *C. falcatum*, may also have a putative role in pathogenicity as an effector during host-pathogen interaction, as predicted by EffectorP.

The abundance of small secreted protein (SSP) in dark-cultured *C. falcatum* was six-fold lesser than the virulent light-culture. The name, SSP merely represent a class of small secreted proteins without any specific functional annotation. Further, BLASTP analysis showed that the obtained hits were annotated as just hypothetical proteins or small secreted proteins. EffectorP tool predicted this protein as a non-effector. Most of the fungal secretome contains a significant percentage of SSPs, which are often species-specific and do not have conserved motifs or domains [44]. Recently, a fungal kingdom-wide analysis of SSPs reported that most of them might be associated with pathogenicity and may act as effectors [45]. Therefore, based on its higher abundance in the virulent light-culture, SSP could possibly be associated with the pathogenicity of *C. falcatum*.

MLP that stands for ML (MD-2-related lipid-recognition) domain-containing protein is basically a lipid recognition protein, present in fungi, plants and animals [46]. This domain was predicted to form a lipid recognition module, similar to immunoglobulin *E*-set domains to interact with specific lipids. This domain may exist either alone or in fusion with some other domains to interact with lipids, lipopolysaccharides, etc. to play diverse range of functions apart from lipid signaling and metabolism [47]. In our study, the abundance of MLP protein was two-fold less in dark-cultured *C. falcatum* and predicted to be an effector by EffectorP. MLP was identified as an effector in *Puccinia graminis* and *Melampsora lini* and reported to play the role of scavenging self-lipopolysachharides, thereby preventing elicitation of host defense [34]. After deliberating these putative roles of MLP in other fungi, prediction of a putative membrane binding domain and higher abundance in the virulent light-culture, it could be inferred that the MLP of *C. falcatum* may play a potential role in membrane-associated infection processes, as an effector.

The abundance of putative glycosyl hydrolase family 10 (GLHY) protein was more than five-fold higher in the virulent light-culture of *C. falcatum*. Biochemically, the basic function of glycosyl hydrolase is to hydrolyse the glycosidic bond between carbohydrate moieties or wherever the bond exists. Biologically, based on substrate specificity, a majority of the glycosyl hydrolase family 10 proteins function as *endo*-β-1,4-xylanases, while some may function as endo-1,3-β-xylanase and cellobiohydrolase [48]. Xylan is a major hemicellulose component of plant cell wall. Fungal glycosyl hydrolase family 10 proteins function as endo-β-1,4-xylanase to hydrolyse these xylan into xylanoligosaccharides [49]. Even though, the GLHY was not predicted to be an effector, these proteins are well known to be involved in hydrolysing host cell wall structure for penetration and readjustments, and thus facilitate colonization [50]. Deletion or absence of these endo-β-1,4-xylanases have been shown to affect pathogenicity by reducing disease severity and delaying disease development [50,51]. Contemplating these functions and the abundance of GLHY, it was presumed that GLHY might play an essential role as a virulence determinant of *C. falcatum* during initial infection processes and further colonization.

Similar to SSP, the functional role of HYP1, the exclusively abundant protein of dark-cultured *C. falcatum*, could not be annotated, except for its prediction as an effector by EffectorP tool. As a consequence of absence of light and with less abundance of other pathogenicity determinants, dark-cultured *C. falcatum* might have employed this new effector in an attempt to balance the loss of virulence.

To understand the functional significance of other identified proteins, namely BYS1, HYP2 and EPL1, which were highly abundant in either light- or dark-cultured *C. falcatum*, their transcript expression was profiled at in vitro culture conditions and at different time points during in planta colonization (0, 12, 24, 48, 72, 120 and 600 hpi), with concurrent quantification of pathogen biomass. Results of the pathogen biomass quantification showed a gradual reduction of dark-cultured *C. falcatum* biomass after 24 h and a complete decline at 600 h, which otherwise indicated a complete elimination of the pathogen (Fig. 6A). On the other side, the light-cultured *C. falcatum* gradually colonized the host until 48 h and increased the pace after 48 h. In *Colletotrichum* spp., this time point coincides with the establishment of secondary hyphae to colonize adjacent cells and marks the transitional shift from biotrophic to necrotrophic phase [52]. Further, an array of stage or phase-specific effectors that mediate the initial infection processes (0–24 h), biotrophic phase (24–48 h), transition phase and necrotrophic phase (> 48 h) were identified in many *Colletotrichum* spp. [42,53]. Mutation of some of these genes have been shown to affect the specific phase and restrict the progression of disease [54]. Similarly, in our study, the failure of dark-cultured *C. falcatum* to colonize progressively after 24 h might be due to the absence or low abundance of some of the identified putative effectors.

Temporal expression profiling of BYS1 transcript showed that the relative expression level has decreased linearly from the in vitro (axenic) culture stage to 72 hpi in in planta and began to increase back only at 600 hpi (Fig. 6B). Although, the identified BYS1 (*Blastomyces* yeast phase-specific 1) family protein is present in many fungal species, it is highly conserved among *Colletotrichum* spp. *Hitherto*, the functional role of BYS1 has not been studied in any phytopathogens. BYS1 was first identified in *Blastomyces* species and so far, it has been characterized only in this species. This gene was found to be expressed only during yeast phase and not during mold phase. Unlike other yeast phase-specific genes viz., BAD1, CBP1, YPS3 and SOWgp, which are essential for virulence, BYS1 is not essential for virulence, but plays a major role in cell wall formation and cell morphology [55]. In our study, the abundance of two BYS1 protein spots, B1 and A5 were exclusively secreted and more than five-fold higher in light-culture, respectively. Similarly, under in vitro conditions, the transcriptional expression of BYS1 was several folds higher in light-culture, wherein visible sporulation has been observed as against the dark-culture that did not exhibit any visible sporulation. Under in planta conditions, its expression was observed only with the light-culture, but reduced linearly in initial stages and resumed back only at 600 hpi. This time point has been correlated with the initiation of sporulation around the external surfaces of nodal root eyes, after extensive colonization of internal tissues. Hence, the expression profile of BYS1 suggested that this protein might be associated with sporulation phase of *C. falcatum*. Meanwhile, the contemplation of

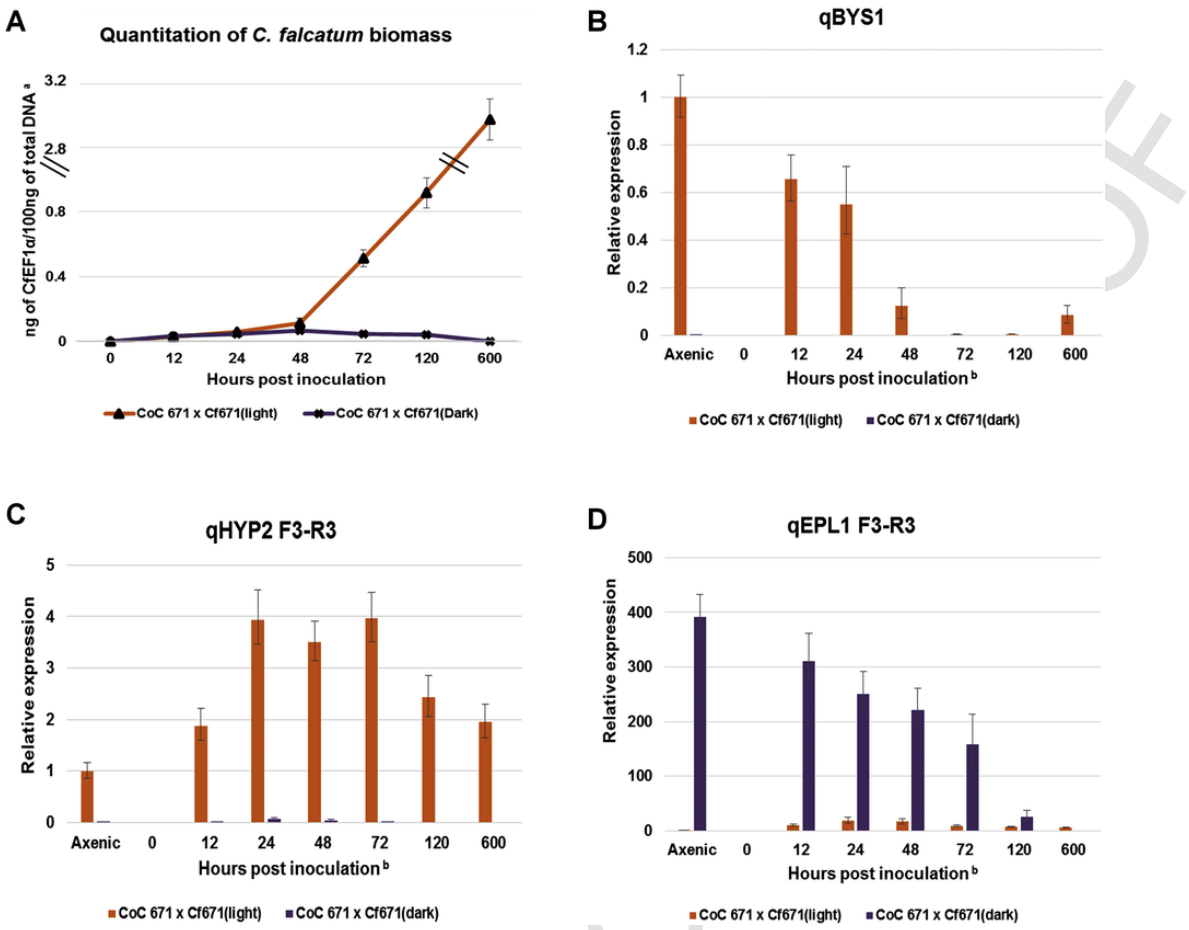

Fig. 6. In planta quantitation of *C. falcatum* biomass and relative transcript expression analysis of a few highly abundant secreted proteins in either light- or dark-cultured *C. falcatum*. A) Temporal quantification of *C. falcatum* biomass by absolute quantification method. [a]Y-axis values were broken (‖) to make the low level of alterations in quantity of dark-cultured *C. falcatum* biomass is visible; (B), (C) and (D) are relative temporal expression of BYS1, HYP2 and EPL1 transcripts, respectively by comparative C_T method. [b]Numerical values in X-axis indicate hours post-inoculation except the in vitro axenic culture. '0 h' indicates mock inoculated control. Error bars indicate standard deviation of three biological replicates with two technical replicates each.

the results of EffectorP prediction, putative PTM regulation of protein abundance and their transcriptional expression pattern at early stages of colonization have suggested that this protein may also have a significant role in regulating the initial infection processes like appressorial or infection peg formation for penetration into the host cell.

HYP2 protein, which has been represented by a single transcript, but with two different protein species with more than five and three-fold higher abundances in light-culture, might have played a significant role in the pathogenicity of *C. falcatum*. This protein has no > 40% identity hits, when blasted in NCBI protein database. To enhance the fitness and host-specificity during the relentless coevolution of plant-fungal interactions, every pathogen has evolved many species-specific effectors with no or very less homology to the conserved effectors [56]. Hence, to understand the role of this novel protein, which has been predicted with effector properties, the expression of this gene was transcriptionally profiled at different time points of colonization. Results showed that the in planta level of expression was constitutive with light-culture, but with a higher fold of expression between 24 and 72 hpi (Fig. 6C). On the other hand, only a very feeble expression was detected at 24 and 48 hpi in the dark-culture. These results have highlighted that HYP2 might have played a potential role as species-specific effector in establishing primary hyphal colonization, besides other phases of colonization. However, the distinguished roles of the two different protein species of HYP2 could not be determined with this temporal transcriptional profiling alone.

Besides the exclusively secreted HYP1 protein, the only high abundant protein in the dark-culture was EPL1. It was represented by two protein species, one with more than seven-fold higher abundance (A4) and the other with just 1.3 fold higher abundance (A7). EPL1 (eliciting plant response-like protein) was identified in more than fifty filamentous fungi like *Stagnospora nodorum*, *M. oryzae*, *Trichoderma* spp., etc., and belongs to a protein family called cerato-platanin family [57]. EPL1, a small, cysteine-rich protein ranging 120–134 amino acids (without signal peptide) with approximately 12 kDa size was reported to be secreted predominantly in extracellular spaces, while some may be adhered to or localized in fungal cell walls [58,59]. EPL1 along with its homologs and orthologs have been reported to play diverse functional roles, viz., elicitor, phytotoxin and virulence factor during different plant-pathogen interactions (Supplementary Table 5).

In our study, dissection and transcriptional profiling of EPL1 have revealed two isoforms namely, EPL1FL and EPL1 Δ N1–74, which represented A7 and A4 spots, respectively. BLASTP analysis of EPL1FL indicated that the first putative signal peptide domain (1–74 residues) at N-terminal region was not conserved with any of the identified cerato-platanin family proteins, even within the *Colletotrichum* spp. (Supplementary Fig. 5). It was also found to be a

novel additional domain of EPL1, which exists only in the case of *C. falcatum*. Further, this N-terminal region was also predicted to be the mitochondrial membrane targeting sequence. Hence, the isoform, EPL1FL with 1.3 fold higher abundance in dark-culture was considered as *C. falcatum*-specific cerato-platanin and may have a distinct functional role in *C. falcatum*, unlike other EPL1 proteins, characterized so far.

In planta temporal transcriptional profiling of EPL1 showed a several hundred-fold higher expression in dark-culture than light-cultured *C. falcatum*, but continued to decline steadily through the earlier stages of colonization and absent after 400 hpi (Fig. 6D). On the other hand, the expression pattern in light-culture exhibited increments in tens of folds until 48 hpi, and began to decrease after that. Since, EPL1 is a highly conserved molecular signature among the filamentous fungi and is recognized by host receptor to activate defense responses, it was reported to act as a microbe-associated molecular pattern (MAMP) or a PAMP, based on its origin [58,60]. In order to avoid this perception and subsequent induction of host defense, in our study, the highly virulent light-cultured *C. falcatum* might have had a very low abundance of EPL1 protein and this would also be a possible explanation for the steady declination at the transcript level in dark-cultured *C. falcatum* - sugarcane interaction.

Comprehensively, in line with the bilateral objective of identifying PAMPs and effectors of *C. falcatum* under the influence of light, this study has identified two pathogenicity-related proteins (SSP, GLHY), most probable effectors (MEP1, MLP, HYP1, BYS1, HYP2) and a protein with putative dichotomous property of PAMP and effector (EPL1). These pathogenicity determinants could either secrete into apoplastic spaces or into the cytoplasm of the host during sugarcane - *C. falcatum* interaction. Among these identified proteins, EPL1 has been reported to play a potential role in inducing host defense, disease resistance and activation of mycoparasitism-associated genes in many hosts. Based on gene knockout experiments and other functional assays, this gene has been demonstrated to play two important roles. First one was a primary role in growth and development of the fungi, as hypothetically played by cell wall adhered or bound EPL1 [59] and the second one was an elusive role of both as a PAMP or an effector during plant-fungal interactions played by secreted EPL1 proteins [60]. Hence, EPL1 has been investigated further for its functional properties as an inducer of defense and disease resistance in the model plant, *N. tabacum* and sugarcane with recombinant EPL1 proteins.

3.6. Production and physical characterization of recombinant EPL1 proteins

Structurally, EPL1 is a non-catalytic, but a highly stable protein over a wide range of pH and temperature [58]. It has a unique combination of physical and biological properties of expansins and hydrophobins. Precisely, similar to expansins, EPL1 proteins have carbohydrate (chitin) binding or loosening properties [61], while on the other hand, similar to hydrophobins, it has a higher tendency to form aggregates or protein layers by self-assembling at air-water interfaces or hydrophobic/hydrophilic interfaces, and alter the polarity of the surfaces or solution [28,62]. In fact, this chitin binding property of EPL1 reiterates its localization in fungal cell wall. In some filamentous fungi, the dimerized form of EPL1 has been shown to negatively impact its elicitor activity. For instance, in *Trichoderma virens*, Sm1, a homolog of EPL1, secreted in the form of a monomeric glycoprotein could elicit host defense. On the contrary, the dimeric form of Sm1 lacked the N-glycosyl moiety at the 29th residue in DNGSR motif (a putative motif that can be recognized by the fungal glycosylation machinery) could not induce host resistance [63].

Multiple sequence alignment of the well conserved isoform, EPL1 Δ N1–74 with other functionally characterized EPL1 proteins showed that CfEPL1 (EPL1 Δ N1–74) have a cysteine at the 58th residue, in addition to the conserved four cysteine residues (Supplementary Fig. 6a). Further, phylogenetic analysis showed that CfEPL1 was closely related to the well characterized *M. oryzae* EPL1 ortholog (SnodProt1), next to *Colletotrichum* spp. (Supplementary Fig. 6b). These analyses have also inferred that unlike the orthologs of EPL1 of *T. virens* and the closely related *C. sublineola*, CfEPL1 did not possess the N-glycosylation motif. More specifically, aspartic acid (D) was present at the 29th residue of CfEPL1, instead of asparagine (N). The results of this analysis suggested that CfEPL1 would not be a glycoprotein. However, to ensure this assumption, the native LMW secreted proteins from dark-cultured *C. falcatum* was electrophoresed using SDS-PAGE and stained with Pierce™ Glycoprotein staining kit (ThermoFisher Scientific, USA). As expected, the results did not show presence of glycoproteins, especially at the range of MW of EPL1 (Fig. 7A). With this experimental validation, it was decided to produce recombinant EPL1 proteins through a bacterial expression system for functional characterization.

For cloning and expression of CfEPL1, three different target sequences namely, EPL1FL, EPL1 Δ N1–74 and EPL1 Δ N1–92 (Fig. 5B) were constructed in a bacterial expression vector, pET28a and expressed in Rosetta™ 2(DE3)pLysS cells. The recombinant proteins were then purified using Ni Sepharose 6 Fast Flow column (GE Healthcare) and Sephacryl S200 HR column. Even after two stages of purification, more than one band was detected for all three EPL1 products (Fig. 7B). Subsequent analysis with Western blot indicated that the bands other than the target size were their dimeric and tetrameric forms, respectively. Our attempts to reduce these dimeric and tetrameric forms to monomer by subjecting them to thermal stress of up to 95 °C for 5 min, strong reducing environment with 700 mM of β-Mercaptoethanol or 300 mM of DTT did not increase the proportion of monomer. On the other hand, an attempt to purify the monomeric forms were futile, since, a significant proportion of the purified monomers were again converted to dimeric and tetrameric forms.

Interestingly, one more physical property that was observed uniformly in all three products was self-assembling at air-water interfaces. Microscopic observation of a drop of these protein solutions (50 ng/μL) in a glass sides, after 2 h at room temperature showed formation of micro globular crystal structures (Fig. 8A). In other words, microbubbles formed during pipetting of EPL1 protein solutions were self-stabilized as irregularly crinkled globular crystal structures due to the self-assembling property at air-water interfaces. And, possibly to support the formation of self-assembled layers in the interface structure of air bubble, a small hole was created and facing upwards (air surface). Similar kind of globular crystal structures caused by small air bubbles exhibited by the self-assembling property were reported earlier in the case of EPL1 of *T. atroviride* [28]. Altogether, these observations have reinstated the physical properties of cerato-platanin proteins and also demonstrated that the N-terminal region (1–92 residues) is dispensable for heat stability, dimer, tetramer formations and self-assembling properties. However, the modelling of three dimensional structure of EPL1 (Fig. 8E) showed that the active carbohydrate binding region, β1 strand (93–114 residues) [61], starts immediately to the downstream of putative signal peptides (1–92 residues). This has indicated that the EPL1 protein products, EPL1FL and EPL1 Δ N1–74 that have additional N-terminal domains up-

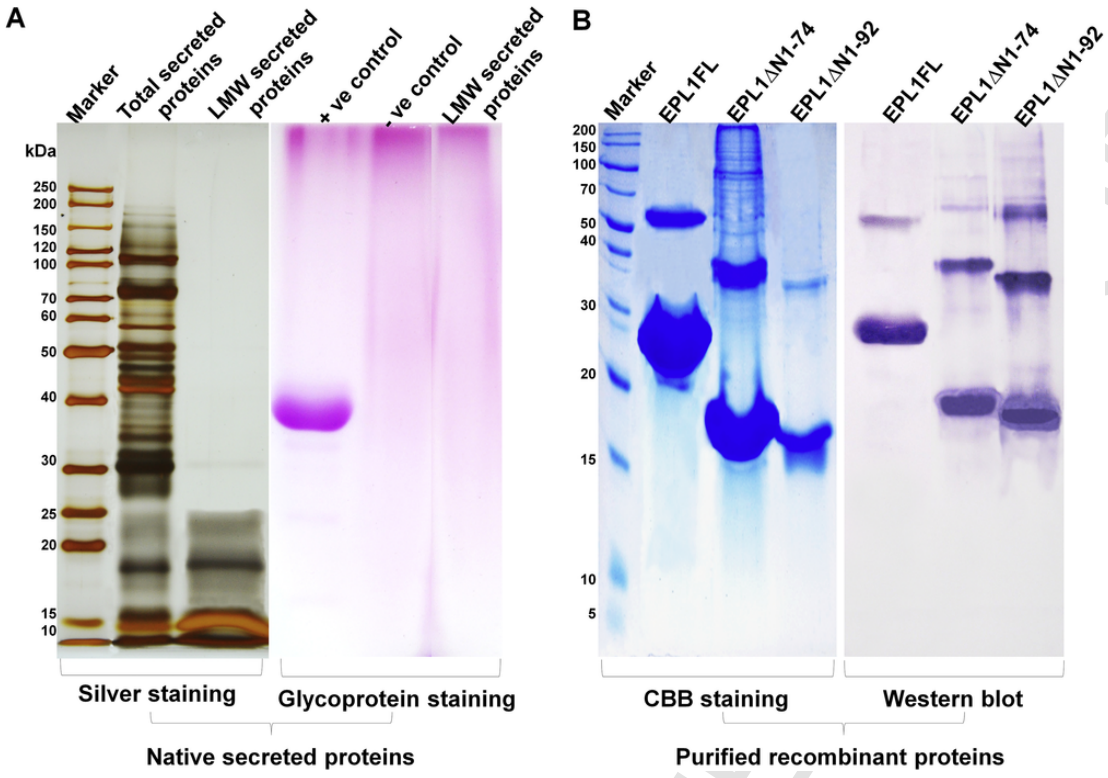

Fig. 7. SDS-PAGE profiles of native secreted proteins of dark-cultured *C. falcatum* and recombinant EPL1 proteins. A) Profiles showing total secreted proteins and low molecular weight (LMW) secreted proteins stained with silver staining and glycoprotein staining. For positive control and negative control, Horseradish peroxidase and Soybean trypsin inhibitor were used, respectively; B) In vitro expressed and purified full length and domain deleted recombinant EPL1 proteins exhibiting monomer, dimer and tetramer forms in CBB stained SDS-PAGE profile and in Western blot detection with T7 tag antibody (Merck Millipore).

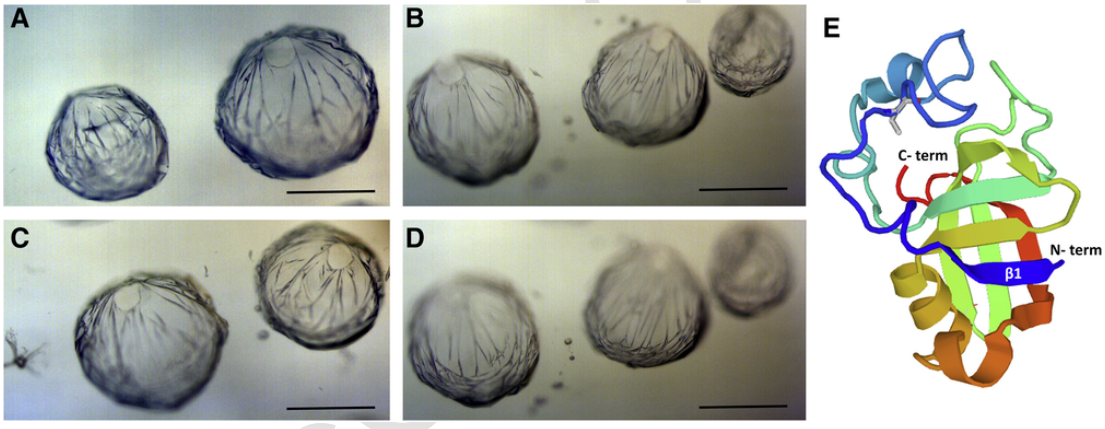

Fig. 8. Observation of putative self-assembled crystal structures of recombinant EPL1 Δ N1–92 under light microscope at different focal planes. Microbubbles formed during pipetting of EPL1 protein solutions on a glass side were self-stabilized as irregularly crinkled globular crystal structures because of the self-assembling property of EPL1. A, B, C represent different bubble structures, whereas B and D represent same bubble structures but at varying focal length to show the differences in crinkled self-assembled layers. Bar indicates 100 μm; E) 3D structure modelling of CfEPL1 (EPL1 Δ N1–92) using SwissModel tool. Blue colored region represent the carbohydrate active perturbation and chemical shift residues present immediately at N-terminal region. (For interpretation of the references to color in this figure legend, the reader is referred to the web version of this article.)

stream to the β1 strand may have a significant impact on carbohydrate binding property.

3.7. Functional analysis of recombinant EPL1 proteins

Generally, plants resist the attack of pathogens by evoking a series of early defense responses, which lead to the activation of its robust innate immune system. As soon as plants perceive the presence of a pathogen by recognizing its PAMPs, it initiates a series of early defense actions like MAPK signaling, extracellular alkalinization, production of reactive oxygen species (ROS), oxidative burst, etc. [64].

In our study, to evaluate the major functional property of EPL1 as a PAMP eliciting host defense, the three different recombinant CfEPL1 proteins were subjected to bioassays such as extracellular alkalinization measurement and detection of H_2O_2 production in sugarcane suspension cells. To optimize the minimum concentration that can induce host defense, 50 μL of different concentrations (0, 25, 50, 75, 100 ng/μL) of native LMW fraction was added to sugarcane sus-

pension culture (cv. CoC 671) and the increments in extracellular pH for 3 h at different time points were observed. Results indicated that 50 ng/μL concentration was the minimum concentration inducing rapid alkalinization as comparable with 75 and 100 ng/μL concentration (Data not shown). Therefore, 50 ng/μL protein concentration was used for all functional bioassays involving native LMW proteins of dark-culture and recombinant EPL1 proteins. Initially, native LMW proteins of dark-culture was used as a positive control for few bioassays.

Extracellular pH measurement of recombinant EPL1 proteins showed that EPL1 Δ N1–92 induced a rapid alkalinization in the first 10 min and reached to a maximum pH of 6.7 at 180 min post-treatment than any other recombinant EPL1 proteins and native LMW proteins (Fig. 9A). Among the three EPL1 proteins, EPL1FL induced a least increment in pH, while the pattern of pH increment of EPL1 Δ N1–74 was relatively lesser to the native LMW fraction. Subsequent detection of H_2O_2 production at 24 h post-treatment by DAB staining indicated that except EPL1FL, the other two EPL1 proteins and native LMW fraction have produced a detectable quantity of H_2O_2 (Fig. 9B). Oxidative burst is one of the early defense responses of plants against pathogen attack and are induced by elicitor treatments. ROS, especially superoxides and H_2O_2 are the toxic intermediates formed during the reduction of molecular oxygen to counterattack pathogen invasion [65]. Hence, our preliminary results suggested that the recombinant EPL1 proteins essentially mimicked as a PAMP of *C. falcatum* and elicited different levels of host defense. Further, it has suggested that the presence of the putative signal peptide domains 1 and 2 at the N-terminal of main cerato-platanin domain might have significantly affected the perception of the EPL1 and so as the level of defense induction in sugarcane suspension cells.

Elicitor induced ROS production results in subsequent defense responses like cell wall reinforcement, HR, activation of defense gene expression [29,66,67]. Tobacco is often used as a model system to study these defense responses, especially the development of HR. Therefore, in another bioassay, the recombinant EPL1 products were infiltrated on *N. tabacum* leaves and observed for the development of HR and H_2O_2 production. Results showed that only EPL1 Δ N1–74 and EPL1 Δ N1–92 were able to induce HR development and H_2O_2 production at 24 h post-infiltration (Fig. 9C and D). Unlike sugarcane suspension cells, native LMW fraction failed to induce HR and H_2O_2 production in tobacco leaves, even with higher concentrations. It was interesting to note that only the recombinant EPL1 proteins induced HR, but not the native EPL1 present in LMW fraction. Besides, the differences in the degree of defense induction in sugarcane and tobacco, reinstate the fact that the perception of PAMPs are dependent on host genotype. Overall, these bioassays have demonstrated that EPL1 Δ N1–92 induces maximum defense, when compared to the other two EPL1 proteins and could act as a potential resistance inducer in both sugarcane and tobacco. Therefore, EPL1 Δ N1–92 was used for further functional assays in sugarcane.

3.8. EPL1 Δ N1–92, a potential PAMP inducing systemic resistance in sugarcane

To evaluate the efficacy of CfEPL1 as a resistance inducer in sugarcane, eight-month old sugarcane were primed with EPL1 Δ N1–92 by foliar spray method and challenged with *C. falcatum*. Priming efficacy was determined by examining the disease severity in both leaves and cane stalks by detached leaf assay and plug inoculation method, respectively. Meanwhile, EPL1 Δ N1–92 was co-infiltrated with *C. falcatum* spores on non-primed leaves to mimic the effect of over expression of EPL1. Detached leaf assay did not show significant differences in appressorium formation between control and primed leaves at 24 hpi, but the rate of disease progression and severity was considerably reduced in primed leaves (Fig. 10A and B). In the co-infiltrated leaves, the germinated hyphal structures were highly melanized, while the number of appressorium formation was reduced (Fig. 10A). However, there were no differences in disease severity between the control and co-infiltrated leaves.

Appressorial structures are the specialized infection structures of pathogens that aid in penetrating the cell wall of the host with higher turgor pressure [68]. The turgor pressure exerted by the appressorium is directly proportional to the presence of an external melanin layer and so the penetration efficiency [69,70]. On the other hand, formation of germ tube, appressorial structures and their melanization is largely dependent on cell surface, hydrophobicity, etc. [70]. Further, the melanization of appressoria and hyphae are mediated by the accumulation of highly osmotic solutes like glycerol [69,71]. Melaniza-

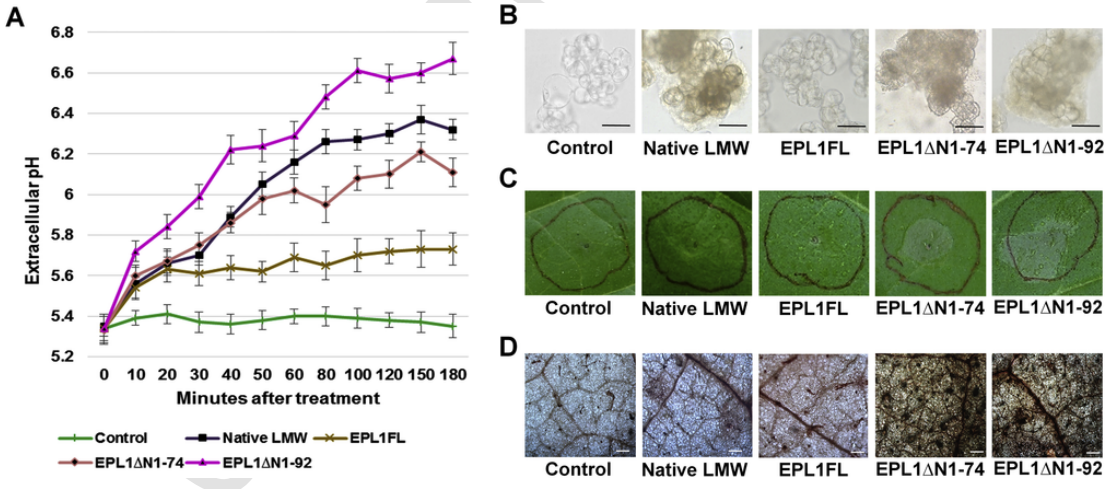

Fig. 9. CfEPL1 treatment on sugarcane suspension cells and *N. tabacum*. A) Induction of extracellular alkalinization by EPL1 protein species in sugarcane cv. CoC 671 suspension cells; B) Microscopic observation of H_2O_2 accumulation in sugarcane cv. CoC 671 suspension cells by DAB staining at 24 h post-treatment of EPL1 protein species. Bar indicates 50 μm; C) Induction of HR on *N. tabacum* leaves by EPL1 protein species at 24 h post-infiltration; D) Microscopic observation of H_2O_2 accumulation at the site of EPL1 protein species infiltration on *N. tabacum* leaves using DAB staining method. Bar indicates 100 μm. Assay buffer was used for control. Native LMW denotes native LMW secreted protein fraction of dark-cultured *C. falcatum*.

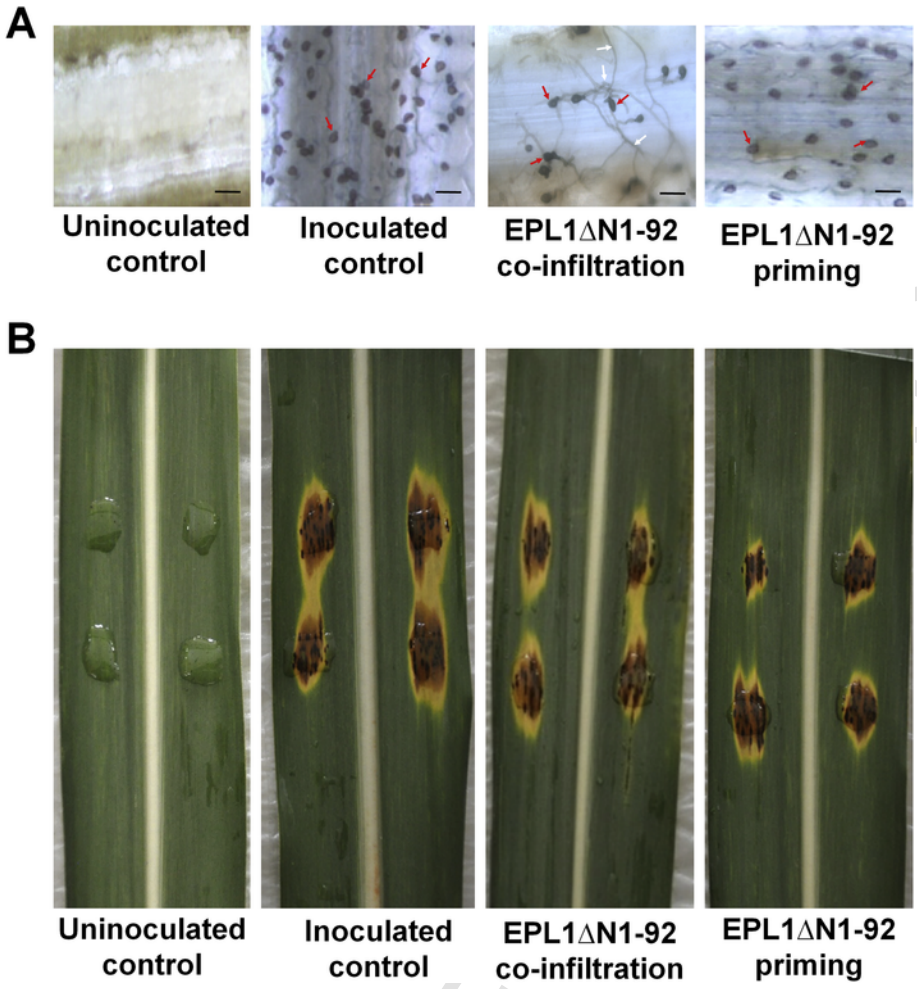

Fig. 10. Observation of co-infiltration and priming effect of EPL1 Δ N1–92 on sugarcane leaves by detached leaf assay method. A) Microscopic observation at 24 h post-inoculation. Bar indicates 10 μm. Red and white arrows indicate appressorial and melanized hyphal structures of *C. falcatum*, respectively; B) Phenotypic observation at 72 h post-inoculation. Brown and yellow lesion indicates the degree of pathogen colonization and their consequent senescence effect, respectively. (For interpretation of the references to color in this figure legend, the reader is referred to the web version of this article.)

tion has many roles like protection of fungal structures against many external stresses, aiding the attachment of conidia and hyphal structures to host cell wall, induction of virulence factors to facilitate penetration, etc. [72]. In this study, the relatively less number of appressorial formation associated with hyphal melanization observed with the co-infiltration of EPL1 Δ N1–92 suggested that the polarity altering property of EPL1 on host cell surface might have affected the appressorium frequency, while inducing rapid melanization of germinated hyphae. Similarly, the same melanization along with the biophysical properties of EPL1 might have increased the penetration efficiency of appressoria [73] and so, the disease severity remained unaffected. This assay has established that EPL1 Δ N1–92 priming essentially played the role of PAMP and as a resistance inducer, which was evident from the suppression of disease severity. Besides, to assess the efficacy of EPL1 Δ N1–92 in inducing systemic resistance at molecular level, foliar primed canes were pathogen challenged by plug inoculation method and the expression of a few candidate defense genes associated with systemic resistance were evaluated with their concomitant pathogen biomass. Pathogen biomass quantification analysis indicated a reduction of pathogen biomass in primed canes, since 72 hpi and showed a significant suppression of pathogen biomass at 600 hpi (Fig. 11A). This analysis has clearly demonstrated the effect of systemic resistance induced by EPL1 Δ N1–92 priming.

Induction of systemic resistance is associated with the expression of the master regulator gene, Non-expressor of pathogenesis-related genes 1 (NPR1) and other PR proteins [74]. Therefore, a few potential candidate defense genes associated with systemic resistance, viz., NPR1, β-1,3-glucanase D (PR2) and chitinase VII (PR3) were analyzed further. Results of expression profiling showed that the priming with EPL1 Δ N1–92 has activated the defense mechanism by inducing the expression of all these defense genes, as observed at 0 hpi (Fig. 11B, C and D). Specifically, the expression of NPR1 has increased by eighteen-fold after priming, which gradually decreased after pathogen inoculation. On the other hand, the expression of NPR1 in untreated control increased only after 72 hpi, by the time *C. falcatum* could have transitioned to necrotrophic phase. The expression level of the PR proteins such as β-1,3-glucanase D and chitinase VII were also increased with response to priming and at early stages of colonization, after which they were intermittently regulated in line with dynamic colonization.

PR proteins are a group of inducible defense-related proteins that are produced in response to pathogen attack or with the application of elicitors or resistance inducers [75]. Chen et al. [76] reported upregu-

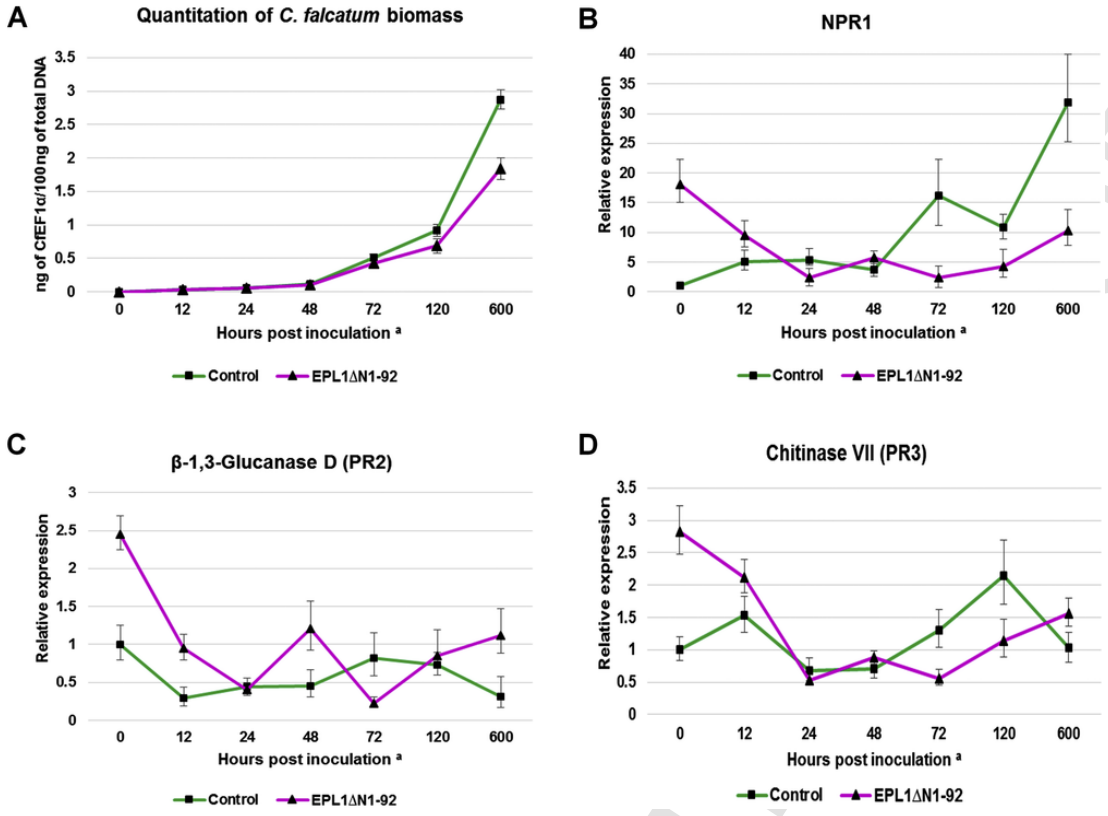

Fig. 11. Quantitation of *C. falcatum* biomass and relative expression analysis of a few candidate defense-related genes in EPL1 Δ N1–92 primed sugarcane stalks. '0 h' indicates primed mock inoculated control. For inoculation light-cultured *Cf*671 was used.

lated expression of sugarcane NPR1 (NPR1) at early intervals in smut resistant cultivars and the expression was found to be positively regulated with response to salicylic acid application, and thus the study has demonstrated the likely involvement of NPR1 in the induction of systemic resistance. In our study, a higher level of expression of NPR1 was observed due to the priming with EPL1 Δ N1–92. This phenomenon of earlier expression of NPR1, even before the perception of the pathogen might have led to the downstream signaling of higher expression of PR genes such as β-1,3-glucanase, chitinase VII at the early hours of host-pathogen interaction (0 to 12 hpi). Over the years, many reports have highlighted the potential role of PR proteins in conferring disease resistance in sugarcane. Viswanathan et al. [30] reported that the abundant expression of chitinases and β-1,3-glucanases are playing a major role in restriction of pathogen colonization during incompatible interaction in sugarcane. Differential expression analysis of sugarcane - *C. falcatum* interaction using DD-RT-PCR and suppression subtractive hybridization (SSH) revealed two-fold higher expression of β-1,3-glucanase, chitinase and PR10 genes at early intervals (0 to 48 h post-inoculation) during incompatible interaction [77,78].

Contemplating these reports with the obtained results, it could be asserted that EPL1 Δ N1–92 induced systemic resistance against *C. falcatum* in sugarcane, thereby significantly suppressed the red rot ~~disease~~ severity. Hence, it is suggested that CfEPL1 can be effectively employed for practical application, as it obviates the issues like lack of sequence information, difficulties in mass production, etc. that were confronted earlier with the glycoprotein elicitor. Nevertheless, before proceeding with the practical application, an assessment on several other factors like cost of mass production, fitness (allocation) costs, trade off issues with beneficial microbial interactions and environmental toxicity is necessary.

4. Conclusion

Comprehensively, in line with the bilateral objective of identifying both PAMP and effector of *C. falcatum*, this study has identified putative effectors, pathogenicity determinants and a PAMP. Although many studies have highlighted the importance of light for the expression of photoreceptors and production of melanin, which in turn is associated with pathogenicity, the direct role of light in the expression of virulence factors like effectors have not been established, so far. For the first time, here we established a direct link between light and the expression of effectors and other pathogenicity related proteins. Substantially, the low abundance of effectors and other pathogenicity related proteins were corroborated with the attenuated pathogenicity of dark-cultured *C. falcatum* in sugarcane. Besides, we have characterized the physical and biological properties of distinct domains of the EPL1 protein and demonstrated that EPL1 Δ N1–92 induces HR in tobacco and systemic resistance against red rot ~~disease~~ in sugarcane. The study has also identified a new isoform of EPL1 with unknown functions. On a futuristic note, the identification of the cognate receptors that recognizes EPL1, and other putative effectors in sugarcane would provide a deeper insight into the sequential events that orchestrate the defense mechanism during sugarcane-filamentous fungus interaction including PTI and ETI responses. This would also help to develop a broad-spectrum of pathogen-derived disease resistance strategy in sugarcane.

Supplementary data to this article can be found online at http://dx.doi.org/10.1016/j.jprot.2017.05.020.

Conflict of interest

The authors declare that the research was conducted in the absence of any commercial or financial relationships that could be construed as a potential conflict of interest.

Acknowledgements

The authors are grateful to The Director, ICAR-Sugarcane Breeding Institute for providing facilities and continuous encouragement. The financial supports received from Department of Science and Technology (DST), New Delhi and Indian Council of Agricultural Research (ICAR), New Delhi are greatly acknowledged. The authors are indebted to INPPO (http://www.inppo.com/) for their support and encouragement.

References

[1] R.P. Singh, S. Lal, Red rot, in: P. Rott, R.A. Bailey, J.C. Comstock, B.J. Croft, J.C. Girard, A.S. Saumtally (Eds.), A Guide to Sugarcane Diseases, Quae, CIRAD, France, 2000, pp. 153–160.
[2] R. Viswanathan, Sugarcane Diseases and their Management, ICAR-Sugarcane Breeding Institute, Coimbatore, India, 2012.
[3] A.R. Sundar, N.M.R. Ashwin, E.L. Barnabas, P. Malathi, R. Viswanathan, Disease resistance in sugarcane – an overview, Sci. Agrar. Parana. 14 (2015) 200–212, http://dx.doi.org/10.18188/1983-1471/sap.v14n4p200-212.
[4] C. Zipfel, Early molecular events in PAMP-triggered immunity, Curr. Opin. Plant Biol. 12 (2009) 414–420.
[5] L. Wu, H. Chen, C. Curtis, Z.Q. Fu, How plants deploy effector-triggered immunity to combat pathogens, Virulence 5 (2014) 710–721.
[6] L. Burketova, L. Trda, P.G. Ott, O. Valentova, Bio-based resistance inducers for sustainable plant protection against pathogens, Biotechnol. Adv. 33 (2015) 994–1004.
[7] B.P.H.J. Thomma, T. Nürnberger, M.H.A.J. Joosten, Of PAMPs and effectors: the blurred PTI-ETI dichotomy, Plant Cell 23 (2011) 4–15.
[8] W.J. Kloepper, S. Tuzun, A.J. Kuc, Proposed definitions related to induced disease resistance, Biocontrol Sci. Tech. 2 (1992) 349–351.
[9] U. Conrath, G.J.M. Beckers, V. Flors, P. García-Agustín, G. Jakab, F. Mauch, M.A. Newman, C.M.J. Pieterse, B. Poinssot, M.J. Pozo, A. Pugin, U. Schaffrath, J. Ton, D. Wendehenne, L. Zimmerli, B. Mauch-Mani, Priming: getting ready for battle, Mol. Plant-Microbe Interact. 19 (2006) 1062–1071.
[10] A. Ramesh Sundar, R. Velazhahan, S. Nagarathinam, P. Vidhyasekaran, Induction of pathogenesis-related proteins in sugarcane leaves and cell-cultures by a glycoprotein elicitor isolated from Colletotrichum falcatum, Biol. Plant. 52 (2008) 321–328.
[11] A. Ramesh Sundar, R. Viswanathan, S. Nagarathinam, Induction of systemic acquired resistance (SAR) using synthetic signal molecules against Colletotrichum falcatum in sugarcane, Sugar Tech 11 (2009) 274–281.
[12] N.M.R. Ashwin, E.L. Barnabas, A. Ramesh Sundar, M. Muthumeena, P. Malathi, R. Viswanathan, Disease suppressive effects of resistance-inducing agents against red rot of sugarcane, Eur. J. Plant Pathol. (2017) http://dx.doi.org/10.1007/s10658-017-1181-1.
[13] M. Muthiah, A. Ramadass, R.S. Amalraj, M. Palaniyandi, V. Rasappa, Expression profiling of transcription factors (TFs) in sugarcane × Colletotrichum falcatum interaction, J. Plant Biochem. Biotechnol. 22 (2013) 286–294.
[14] N. Selvaraj, A. Ramadass, R.S. Amalraj, M. Palaniyandi, V. Rasappa, Molecular profiling of systemic acquired resistance (SAR)-responsive transcripts in sugarcane challenged with Colletotrichum falcatum, Appl. Biochem. Biotechnol. 174 (2014) 2839–2850.
[15] L.C. Roden, R.A. Ingle, Lights, rhythms, infection: the role of light and the circadian clock in determining the outcome of plant-pathogen interactions, Plant Cell 21 (2009) 2546–2552.
[16] A. Idnurm, S. Crosson, The photobiology of microbial pathogenesis, PLoS Pathog. 5 (2009) 11–13.
[17] P. Canessa, J. Schumacher, M.A. Hevia, P. Tudzynski, L.F. Larrondo, Assessing the effects of light on differentiation and virulence of the plant pathogen Botrytis cinerea: characterization of the white collar complex, PLoS One 8 (2013), e84223.
[18] S. Yu, G. Ramkumar, Y.H. Lee, Light quality influences the virulence and physiological responses of Colletotrichum acutatum causing anthracnose in pepper plants, J. Appl. Microbiol. 115 (2013) 509–516.
[19] P. Singh, Effect of light, temperature and substrate during spore formation on the germinability of conidia of Colletotrichum falcatum, Physiol. Plant. 29 (1973) 194–197.
[20] R. Viswanathan, R. Samiyappan, Induction of systemic resistance by plant growth promoting rhizobacteria against red rot disease in sugarcane, Sugar Tech. 1 (1999) 67–76.
[21] E.L. Barnabas, N.M.R. Ashwin, K. Kaverinathan, A.R. Trentin, M. Pivato, A. Ramesh Sundar, P. Malathi, R. Viswanathan, P. Carletti, G. Arrigoni, A. Masi, G.K. Agrawal, R. Rakwal, In vitro secretomic analysis identifies putative pathogenicity - related proteins of Sporisorium scitamineum - the sugarcane smut fungus, Fungal Biol. 121 (2016) 199–211.
[22] R.S. Amalraj, N. Selvaraj, G.K. Veluswamy, R.P. Ramanujan, R. Muthurajan, M. Palaniyandi, G.K. Agrawal, R. Rakwal, R. Viswanathan, Sugarcane proteomics: establishment of a protein extraction method for 2-DE in stalk tissues and initiation of sugarcane proteome reference map, Electrophoresis 31 (2010) 1959–1974.
[23] N. Dyballa, S. Metzger, Fast and sensitive colloidal coomassie G-250 staining for proteins in polyacrylamide gels, J. Vis. Exp. 30 (2009) 2–5.
[24] L. Barnabas, N.M.R. Ashwin, K. Kaverinathan, A.R. Trentin, M. Pivato, A.R. Sundar, P. Malathi, R. Viswanathan, O.B. Rosana, K. Neethukrishna, P. Carletti, G. Arrigoni, A. Masi, G.K. Agrawal, R. Rakwal, Proteomic analysis of a compatible interaction between sugarcane and Sporisorium scitamineum, Proteomics 16 (2016) 1111–1122.
[25] J. Sperschneider, D.M. Gardiner, P.N. Dodds, F. Tini, L. Covarelli, K.B. Singh, J.M. Manners, J.M. Taylor, EffectorP: predicting fungal effector proteins from secretomes using machine learning, New Phytol. 210 (2016) 743–761.
[26] C.F. Diguta, S. Rousseaux, S. Weidmann, N. Bretin, B. Vincent, M. Guilloux-Benatier, H. Alexandre, Development of a qPCR assay for specific quantification of Botrytis cinerea on grapes, FEMS Microbiol. Lett. 313 (2010) 81–87.
[27] H. Ling, Q. Wu, J. Guo, L. Xu, Y. Que, Comprehensive selection of reference genes for gene expression normalization in sugarcane by real time quantitative RT-PCR, PLoS One 9 (2014), e97469.
[28] A. Frischmann, S. Neudl, R. Gaderer, K. Bonazza, S. Zach, S. Gruber, O. Spadiut, G. Friedbacher, H. Grothe, V. Seidl-Seiboth, Self-assembly at air/water interfaces and carbohydrate binding properties of the small secreted protein EPL1 from the fungus Trichoderma atroviride, J. Biol. Chem. 288 (2013) 4278–4287.
[29] M. Chen, H. Zeng, D. Qiu, L. Guo, X. Yang, H. Shi, T. Zhou, J. Zhao, Purification and characterization of a novel hypersensitive response-inducing elicitor from Magnaporthe oryzae that triggers defense response in rice, PLoS One 7 (2012), e37654.
[30] R. Viswanathan, P. Malathi, A. Ramesh Sundar, S. Aarthi, S.M. Premkumari, P. Padmanaban, Differential induction of chitinases and thaumatin-like proteins in sugarcane in response to infection by Colletotrichum falcatum causing red rot disease, J. Plant Dis. Prot. 112 (2005) 417–425.
[31] M. Moline, D. Libkind, M. Del Carmen Dieguez, M. van Broock, Photoprotective role of carotenoids in yeasts: response to UV-B of pigmented and naturally-occurring albino strains, J. Photochem. Photobiol. B Biol. 95 (2009) 156–161.
[32] R. Viswanathan, G.P. Rao, Disease scenario and management of major sugarcane diseases in India, Sugar Tech. 13 (2011) 336–353.
[33] M. Koeck, A.R. Hardham, P.N. Dodds, The role of effectors of biotrophic and hemibiotrophic fungi in infection, Cell. Microbiol. 13 (2011) 1849–1857.
[34] D.G.O. Saunders, J. Win, L.M. Cano, L.J. Szabo, S. Kamoun, S. Raffaele, Using hierarchical clustering of secreted protein families to classify and rank candidate effectors of rust fungi, PLoS One 7 (2012), e29847.
[35] M. Stastna, J.E. Van Eyk, Analysis of protein isoforms: can we do it better?, Proteomics 12 (2012) 2937–2948.
[36] N.M.R. Ashwin, L. Barnabas, A. Ramesh Sundar, P. Malathi, R. Viswanathan, A. Masi, G.K. Agrawal, R. Rakwal, Advances in proteomic technologies and their scope of application in understanding plant–pathogen interactions, J. Plant Biochem. Biotechnol. (2017) http://dx.doi.org/10.1007/s13562-017-0402-1.
[37] B.D. Halligan, V. Ruotti, W. Jin, S. Laffoon, S.N. Twigger, E.A. Dratz, ProMoST (Protein Modification Screening Tool): a web-based tool for mapping protein modifications on two-dimensional gels, Nucleic Acids Res. 32 (2004) 638–644.
[38] I. Saska, D.J. Craik, Protease-catalysed protein splicing: a new post-translational modification?, Trends Biochem. Sci. 33 (2008) 363–368.
[39] S. Elleuche, S. Poggeler, Inteins - selfish elements in fungal genomes, in: T. Anke, D. Weber (Eds.), Physiol. Genet, Springer-Verlag, Berlin Heidelberg, 2009, pp. 41–61.
[40] C.H. Khang, S. Park, Y. Lee, B. Valent, S. Kang, Genome organization and evolution of the AVR-Pita avirulence gene family in the Magnaporthe grisea species complex, Mol. Plant-Microbe Interact. 21 (2008) 658–670.
[41] Y. Jia, S.A. Mcadams, G.T. Bryan, H.P. Hershey, B. Valent, Direct interaction of resistance gene and avirulence gene products confers rice blast resistance, EMBO J. 19 (2000) 4004–4014.
[42] R.J. O'Connell, M.R. Thon, S. Hacquard, S.G. Amyotte, J. Kleemann, M.F. Torres, U. Damm, E.A. Buiate, L. Epstein, N. Alkan, J. Altmüller, L. Alvarado-Balderrama, C.A. Bauser, C. Becker, B.W. Birren, Z. Chen, J. Choi, J.A. Crouch, J.P. Duvick, M.A. Farman, P. Gan, D. Heiman, B. Henrissat, R.J. Howard, M. Kabbage, C. Koch, B. Kracher, Y. Kubo, A.D. Law, M.-H. Lebrun,

Y.-H. Lee, I. Miyara, N. Moore, U. Neumann, K. Nordström, D.G. Panaccione, R. Panstruga, M. Place, R.H. Proctor, D. Prusky, G. Rech, R. Reinhardt, J.A. Rollins, S. Rounsley, C.L. Schardl, D.C. Schwartz, N. Shenoy, K. Shirasu, U.R. Sikhakolli, K. Stüber, S.A. Sukno, J.A. Sweigard, Y. Takano, H. Takahara, F. Trail, H.C. van der Does, L.M. Voll, I. Will, S. Young, Q. Zeng, J. Zhang, S. Zhou, M.B. Dickman, P. Schulze-Lefert, E. Ver Loren van Themaat, L.J. Ma, L.J. Vaillancourt, Lifestyle transitions in plant pathogenic Colletotrichum fungi deciphered by genome and transcriptome analyses, Nat. Genet. 44 (2012) 1060–1065.

[43] J.M. Sanz-Martin, J.R. Pacheco-Arjona, V. Bello-Rico, W.A. Vargas, M. Monod, J.M. Diaz-Minguez, M.R. Thon, S.A. Sukno, A highly conserved metalloprotease effector enhances virulence in the maize anthracnose fungus Colletotrichum graminicola, Mol. Plant Pathol. 17 (2016) 1048–1062.

[44] Q. Cheng, H. Wang, B. Xu, S. Zhu, L. Hu, M. Huang, Discovery of a novel small secreted protein family with conserved N-terminal IGY motif in Dikarya fungi, BMC Genomics 15 (2014) 1–12.

[45] K.T. Kim, J. Jeon, J. Choi, K. Cheong, H. Song, G. Choi, S. Kang, Y.H. Lee, Kingdom-wide analysis of fungal small secreted proteins (SSPs) reveals their potential role in host association, Front. Plant Sci. 7 (2016) 186.

[46] N. Inohara, G. Nuez, ML - a conserved domain involved in innate immunity and lipid metabolism, Trends Biochem. Sci. 27 (2002) 219–221.

[47] M.F. Seidl, G. Van den Ackerveken, F. Govers, B. Snel, A domain-centric analysis of oomycete plant pathogen genomes reveals unique protein organization, Plant Physiol. 155 (2011) 628–644.

[48] S.R. Andrews, S.J. Charnock, J.H. Lakey, G.J. Davies, M. Claeyssens, W. Nerinckx, M. Underwood, M.L. Sinnott, R.A.J. Warren, H.J. Gilbert, Substrate specificity in glycoside hydrolase family 10: tyrosine 87 and leucine 314 play a pivotal role in discriminating between glucose and xylose binding in the proximal active site of Pseudomonas cellulosa xylanase 10A, J. Biol. Chem. 275 (2000) 23027–23033.

[49] T. Collins, C. Gerday, G. Feller, Xylanases, xylanase families and extremophilic xylanases, FEMS Microbiol. Rev. 29 (2005) 3–23.

[50] Q.B. Nguyen, K. Itoh, B. Van Vu, Y. Tosa, H. Nakayashiki, Simultaneous silencing of endo-β-1,4 xylanase genes reveals their roles in the virulence of Magnaporthe oryzae, Mol. Microbiol. 81 (2011) 1008–1019, http://dx.doi.org/10.1111/j.1365-2958.2011.07746.x.

[51] N. Brito, J.J. Espino, C. González, , Mol. Plant-Microbe Interact. 19 (2006) 25–32.

[52] S. Münch, U. Lingner, D.S. Floss, N. Ludwig, N. Sauer, H.B. Deising, The hemibiotrophic lifestyle of Colletotrichum species, J. Plant Physiol. 165 (2008) 41–51.

[53] P. Gan, K. Ikeda, H. Irieda, M. Narusaka, R.J. O'Connell, Y. Narusaka, Y. Takano, Y. Kubo, K. Shirasu, Comparative genomic and transcriptomic analyses reveal the hemibiotrophic stage shift of Colletotrichum fungi, New Phytol. 197 (2013) 1236–1249.

[54] J. Kleemann, L.J. Rincon-Rivera, H. Takahara, U. Neumann, E.V.L. van Themaat, H.C. van der Does, S. Hacquard, K. Stüber, I. Will, W. Schmalenbach, E. Schmelzer, R.J. O'Connell, E. Ver Loren van Themaat, E.V.L. van Themaat, H.C. van der Does, S. Hacquard, K. Stüber, I. Will, W. Schmalenbach, E. Schmelzer, R.J. O'Connell, Sequential delivery of host-induced virulence effectors by appressoria and intracellular hyphae of the phytopathogen Colletotrichum higginsianum, PLoS Pathog. 8 (2012), e1002643.

[55] T. Krajaejun, M. Wüthrich, G.M. Gauthier, T.F. Warner, T.D. Sullivan, B.S. Klein, Discordant influence of Blastomyces dermatitidis yeast-phase-specific gene BYS1 on morphogenesis and virulence, Infect. Immun. 78 (2010) 2522–2528.

[56] P. Schulze-Lefert, R. Panstruga, A molecular evolutionary concept connecting nonhost resistance, pathogen host range, and pathogen speciation, Trends Plant Sci. 16 (2011) 117–125.

[57] H. Chen, S. Kerio, F.O. Asiegbu, Distribution and bioinformatic analysis of the cerato-platanin protein family in Dikarya, Mycologia 105 (2013) 1479–1488.

[58] R. Gaderer, K. Bonazza, V. Seidl-Seiboth, Cerato-platanins: a fungal protein family with intriguing properties and application potential, Appl. Microbiol. Biotechnol. 98 (2014) 4795–4803.

[59] E.V. Gomes, M.D.N. Costa, R.G. de Paula, R. Ricci de Azevedo, F.L. da Silva, E.F. Noronha, C. José Ulhoa, V. Neves Monteiro, R. Elena Cardoza, S. Gutiérrez, R. Nascimento Silva, The Cerato-Platanin protein Epl-1 from Trichoderma harzianum is involved in mycoparasitism, plant resistance induction and self cell wall protection, Sci. Rep. 5 (2015) 17998.

[60] L. Pazzagli, V. Seidl-Seiboth, M. Barsottini, W.A. Vargas, A. Scala, P.K. Mukherjee, Cerato-platanins: elicitors and effectors, Plant Sci. 228 (2014) 79–87.

[61] A.L. de Oliveira, M. Gallo, L. Pazzagli, C.E. Benedetti, G. Cappugi, A. Scala, B. Pantera, A. Spisni, T.A. Pertinhez, D.O. Cicero, The structure of the elicitor cerato-platanin (CP), the first member of the CP fungal protein family, reveals a double ψβ-barrel fold and carbohydrate binding, J. Biol. Chem. 286 (2011) 17560–17568.

[62] K. Bonazza, R. Gaderer, S. Neudl, A. Przylucka, G. Allmaier, I.S. Druzhinina, H. Grothe, G. Friedbacher, V. Seidl-Seiboth, The fungal cerato-platanin protein EPL1 forms highly ordered layers at hydrophobic/hydrophilic interfaces, Soft Matter 11 (2015) 1723–1732.

[63] W.A. Vargas, S. Djonović, S.A. Sukno, C.M. Kenerley, Dimerization controls the activity of fungal elicitors that trigger systemic resistance in plants, J. Biol. Chem. 283 (2008) 19804–19815.

[64] S. Lehmann, M. Serrano, F. L'Haridon, S.E. Tjamos, J.P. Metraux, Reactive oxygen species and plant resistance to fungal pathogens, Phytochemistry 112 (2015) 54–62.

[65] F. Van Breusegem, J. Bailey-Serres, R. Mittler, Unraveling the tapestry of networks involving reactive oxygen species in plants, Plant Physiol. 147 (2008) 978–984.

[66] B. Wang, X. Yang, H. Zeng, H. Liu, T. Zhou, B. Tan, J. Yuan, L. Guo, D. Qiu, The purification and characterization of a novel hypersensitive-like response-inducing elicitor from Verticillium dahliae that induces resistance responses in tobacco, Appl. Microbiol. Biotechnol. 93 (2012) 191–201.

[67] Y.H. Chang, H.Z. Yan, R.F. Liou, A novel elicitor protein from Phytophthora parasitica induces plant basal immunity and systemic acquired resistance, Mol. Plant Pathol. 16 (2015) 123–136.

[68] H.B. Deising, S. Werner, M. Wernitz, The role of fungal appressoria in plant infection, Microbes Infect. 2 (2000) 1631–1641.

[69] K.P. Dixon, J.R. Xu, N. Smirnoff, N.J. Talbot, Independent signaling pathways regulate cellular turgor during hyperosmotic stress and appressorium-mediated plant infection by Magnaporthe grisea, Plant Cell 11 (1999) 2045–2058.

[70] L.A. Kong, G.T. Li, Y. Liu, M.G. Liu, S.J. Zhang, J. Yang, X.Y. Zhou, Y.L. Peng, J.R. Xu, Differences between appressoria formed by germ tubes and appressorium-like structures developed by hyphal tips in Magnaporthe oryzae, Fungal Genet. Biol. 56 (2013) 33–41.

[71] J. de Jong, B. McCormack, N. Smirnoff, N. Talbot, Glycerol generates turgor in rice blast, Nature 389 (1997) 244.

[72] M. Pihet, P. Vandeputte, G. Tronchin, G. Renier, P. Saulnier, S. Georgeault, R. Mallet, D. Chabasse, F. Symoens, J.-P. Bouchara, Melanin is an essential component for the integrity of the cell wall of Aspergillus fumigatus conidia, BMC Microbiol. 9 (2009) 177.

[73] I. Baccelli, Cerato-platanin family proteins: one function for multiple biological roles?, Front. Plant Sci. 5 (2014) 769.

[74] K.M. Pajerowska-Mukhtar, D.K. Emerine, M.S. Mukhtar, Tell me more: roles of NPRs in plant immunity, Trends Plant Sci. 18 (2013) 402–411.

[75] J. Sels, J. Mathys, B.M.A. De Coninck, B.P.A. Cammue, M.F.C. De Bolle, Plant pathogenesis-related (PR) proteins: a focus on PR peptides, Plant Physiol. Biochem. 46 (2008) 941–950.

[76] J. Chen, J. Kuang, G. Peng, S. Wan, R.U.I. Liu, Molecular cloning and expression analysis of a NPR1 gene from sugarcane, Pak J. Botany. 44 (2012) 193–200.

[77] P.T. Prathima, M. Raveendran, K.K. Kumar, P.R. Rahul, V.G. Kumar, R. Viswanathan, A.R. Sundar, P. Malathi, D. Sudhakar, P. Balasubramaniam, Differential regulation of defense-related gene expression in response to red rot pathogen Colletotrichum falcatum infection in sugarcane, Appl. Biochem. Biotechnol. 171 (2013) 488–503.

[78] M. Sathyabhama, R. Viswanathan, M. Nandakumar, P. Malathi, A. Ramesh Sundar, Understanding sugarcane defence responses during the initial phase of Colletotrichum falcatum pathogenesis by suppression subtractive hybridization (SSH), Physiol. Mol. Plant Pathol. 91 (2015) 131–140.